

# **Synthesis of Cyclodextrin-Complexed Metal Carbonyl Polymers**

by

Na Zhou

A thesis

presented to the University of Waterloo

in fulfillment of the

thesis requirement for the degree of

Master of Science

in

Chemistry

Waterloo, Ontario, Canada, 2016

© Na Zhou 2016

## **Author's Declaration**

I hereby declare that I am the sole author of this thesis. This is a true copy of the thesis, including any required final revisions, as accepted by my examiners. I understand that my thesis may be made electronically available to the public.

## Abstract

The synthesis of metal carbonyl (MC) polymers has been explored for decades, but well-defined and well-characterized MC polymers are rarely reported mainly due to the chemical instability of MC complexes. To address this challenge, we explored the host-guest chemistry of cyclodextrins (CDs) with MC complexes and used it to stabilize MC polymers. The MC polymers were prepared *via* the post-polymerization modification of poly(vinylbenzyl chloride) (PVBC) with cyclopentadienyl dicarbonyl iron (Fp) anions. The resulting Fp-PVBC subsequently interacted with  $\beta$ -CDs, generating  $\beta$ -CD-complexed Fp-PVBC ( $\beta$ -CD/Fp-PVBC). Compared with Fp-PVBC, the stability of  $\beta$ -CD/Fp-PVBC was significantly improved. The chemical structure of  $\beta$ -CD/Fp-PVBC was characterized using a range of techniques including Fourier transform infrared (FTIR), nuclear magnetic resonance (NMR) spectroscopy, thermogravimetric analysis (TGA) and cyclic voltammetry (CV).

## **Acknowledgements**

I would like to express my sincerest appreciation to Prof. Xiaosong Wang for his supervision.

Prof. Xiaosong Wang continually gave me a lot of constructive suggestions on experiment design, data analysis and academic writing. Without his guidance and supervision, it would have been difficult for me to finish my thesis.

I appreciate my supervisory committee members, Prof. Mario Gauthier and Prof. Jean Duhamel, for their guidance and support during my studies. I also would like to express my special gratitude to Prof. Mario Gauthier for his kind help on my thesis writing and editing.

I would like to thank Kai Cao for his suggestions on my research. Special thanks also go to all my lab mates: Nicholas Lanigan, Nimer Murshid, Dapeng Liu, Diyang Geng, Shaowei Shi, Zhen Zhang.

Last but most importantly, I would like to express my greatest gratitude to my parents for their great help and support. They taught me an optimistic and positive attitude towards life, which is infinitely precious to me.

## Table of Contents

<b>Author's Declaration .....</b>	<b>ii</b>
<b>Abstract.....</b>	<b>iii</b>
<b>Acknowledgements .....</b>	<b>iv</b>
<b>List of Figures.....</b>	<b>ix</b>
<b>List of Schemes.....</b>	<b>xi</b>
<b>List of Symbols and Abbreviations .....</b>	<b>xiii</b>
<b>1. Introduction.....</b>	<b>1</b>
1.1 Metal-containing polymers .....	1
<i>1.1.1 Main-chain MC polymers.....</i>	<i>1</i>
<i>1.1.2 Side-chain MC polymers .....</i>	<i>4</i>
1.2 Cyclodextrin host-guest chemistry .....	8
<i>1.2.1 Cyclodextrins.....</i>	<i>8</i>
<i>1.2.2 CD inclusion compounds of metal complexes .....</i>	<i>11</i>

1.2.3 Polymer-inclusion complexes with CDs .....	14
<b>2. Experimental .....</b>	<b>20</b>
Materials .....	20
Instrumentation .....	21
2.1 Synthesis of poly(vinyl benzyl chloride) (PVBC) .....	23
2.1.1 Synthesis of <i>S</i> -1-dodecyl- <i>S</i> '-( <i>a</i> , <i>a</i> '-dimethyl- <i>a</i> ''-acetic acid) trithiocarbonate (DDAT) .....	23
2.1.2 RAFT homopolymerization of VBC using DDAT .....	24
2.2 Synthesis of cyclopentadienyldicarbonyliron potassium (FpK) .....	25
2.3 Synthesis of Fp-modified VBC (Fp-VBC) .....	25
2.4 Synthesis of Fp-modified PVBC (Fp-PVBC) .....	26
2.5 Synthesis of $\beta$ -CD complexed Fp-VBC ( $\beta$ -CD/Fp-VBC) .....	27
2.6 Synthesis of $\beta$ -CD complexed Fp-PVBC ( $\beta$ -CD/Fp-PVBC) .....	28
2.7 Synthesis of CD complexed Fp <sub>2</sub> ( $\beta$ -CD/Fp <sub>2</sub> ) .....	29
<b>3. Results and discussion .....</b>	<b>31</b>
3.1 Synthesis of Fp-PVBC .....	31

3.2 Synthesis of $\beta$ -CD/Fp-VBC .....	35
3.3 Synthesis of $\beta$ -CD/Fp-PVBC.....	40
<b>4. Conclusion .....</b>	<b>53</b>
<b>5. Future Work.....</b>	<b>54</b>
<b>References.....</b>	<b>56</b>

## List of Figures

Figure 1. Chemical structures of $\alpha$ -CD, $\beta$ -CD and $\gamma$ -CD. <sup>[24]</sup> .....	9
Figure 2. TGA curves for $Mn_2(CO)_{10}$ (----), its 1:1 $\gamma$ -CD inclusion compounds (—), $\gamma$ -CD (— —) and 1:1 mixture of $Mn_2(CO)_{10}$ and $\gamma$ -CD (— · — · —). <sup>[38]</sup> .....	13
Figure 3. The crystal structure of $\alpha$ -CD complexed PEG. <sup>[49]</sup> .....	15
Figure 4. Synthesis of $\beta$ -CD complexed APN- <i>b</i> -PS diblock copolymers and their micelle formation. <sup>[51]</sup> .....	16
Figure 5. The aqueous solution of $\beta$ -CD complexed PVFc (a); the solution is mixed with hydrogen peroxide and heated to 50 °C (b); orange precipitates are observed (c). <sup>[28]</sup> .....	18
Figure 6. FTIR spectra for PVBC (a) and Fp-PVBC (b). (note: Fp-PVBC contains cross-linked materials).....	33
Figure 7. <sup>1</sup> H NMR spectra (CDCl <sub>3</sub> ) for PVBC (a) and Fp-PVBC (b). .....	34
Figure 8. Photographs for $\beta$ -CD/Fp-VBC solids (a); DMSO solutions of $\beta$ -CD/Fp-VBC (left) and Fp-VBC (right) after storing in air for one month (b). .....	37
Figure 9. TGA curves for $\beta$ -CD/Fp-VBC (solid line), $\beta$ -CD (dashed line) and Fp-VBC (dash	

dotted line). .....	38
Figure 10. FTIR spectra for Fp-VBC (a), $\beta$ -CD/Fp-VBC (b), $\beta$ -CD (c). .....	39
Figure 11. $^1\text{H}$ NMR spectra ( $\text{DMSO-}d_6$ ) for $\beta$ -CD (a), Fp-VBC (b), $\beta$ -CD/Fp-VBC (c). .....	40
Figure 12. Photographs for $\beta$ -CD/Fp-PVBC solids (a); DMSO solutions of Fp-PVBC (left) and $\beta$ -CD/Fp-PVBC (right) after storing in air for one month. ....	42
Figure 13. TGA curves for $\beta$ -CD/Fp-PVBC (solid line), $\beta$ -CD (dotted line) and Fp-PVBC (dashed line). (note: Fp-PVBC contains cross-linked fractions). ....	43
Figure 14. $^1\text{H}$ NMR spectrum ( $\text{DMSO-}d_6$ ) for Fp-PVBC (a) and $\beta$ -CD/Fp-PVBC (b). ....	45
Figure 15. $^{13}\text{C-}^1\text{H}$ HMQC 2D NMR spectrum for $\beta$ -CD/Fp-PVBC in $\text{DMSO-}d_6$ . ....	46
Figure 16. FTIR spectra for Fp-PVBC (a), $\beta$ -CD/Fp-PVBC (b), Fp <sub>2</sub> (c) and $\beta$ -CD/Fp <sub>2</sub> (c). ....	47
Figure 17. The proposed chemical structure for $\beta$ -CD/Fp-PVBC. ....	47
Figure 18. $^1\text{H}$ NMR spectra ( $\text{DMSO-}d_6$ ) for $\beta$ -CD/Fp-VBC (a), $\beta$ -CD/Fp-PVBC (b) and $\beta$ -CD/Fp <sub>2</sub> (c). ....	49
Figure 19. CV curves for Fp-VBC (a), $\beta$ -CD/Fp-VBC (b), Fp-PVBC (c), $\beta$ -CD/Fp-PVBC (d), Fp <sub>2</sub> (e) and $\beta$ -CD/Fp <sub>2</sub> (f). ....	51

## List of Schemes

Scheme 1. Synthesis of main-chain MC polymers <i>via</i> step-growth polymerization. <sup>[15]</sup> .....	2
Scheme 2. Synthesis of main-chain MC polymers <i>via</i> ROP. <sup>[10]</sup> .....	3
Scheme 3. Synthesis of main-chain MC polymers <i>via</i> MIP. <sup>[17]</sup> .....	4
Scheme 4. Synthesis of transition metal vinylbenzyls <i>via</i> substitution reaction. <sup>[9]</sup> .....	5
Scheme 5. Synthesis of side-chain iron carbonyl polymers <i>via</i> post-polymerization modification. <sup>[23]</sup> .....	6
Scheme 6. Synthesis of side-chain cobalt carbonyl polymers <i>via</i> post-polymerization modification. <sup>[8]</sup> .....	7
Scheme 7. A schematic representation for the inclusion complex formation between CDs and guest molecules (1:1). <sup>[25]</sup> .....	9
Scheme 8. Schematic illustration for the MIR of MC complexes (6) with phosphines and the ligand substitution reaction of $\beta$ -CD complexed MC (8) with phosphines. <sup>[39]</sup> .....	14
Scheme 9. Free radical polymerization of VFc in the presence of $\beta$ -CDs using VA-044 as initiators. <sup>[28]</sup> .....	18

Scheme 10. Synthesis of Fp-PVBC <i>via</i> the post-polymerization modification of PVBC using Fp anions. ....	32
Scheme 11. The possible intramolecular and intermolecular dimerization for Fp-PVBC. ....	33
Scheme 12. Synthesis of $\beta$ -CD/Fp-VBC in water.....	36
Scheme 13. Synthesis of $\beta$ -CD/Fp-PVBC. ....	41
Scheme 14. Synthesis of $\beta$ -CD/Fp <sub>2</sub> in water. ....	49
Scheme 15. The proposed dimerization process of the Fp groups on Fp-PVBC after the addition of $\beta$ -CDs.....	52

## List of Symbols and Abbreviations

Ada	Adamantane
APN- <i>b</i> -PS	Adamantyl polyphosphazene-polystyrene block copolymers
AIBN	Azobisisobutyronitrile
Aliquat 336	Tricaprylylmethylammonium chloride
CD	Cyclodextrin
$\beta$ -CD/FCA <sup>-</sup>	$\beta$ -Cyclodextrin-complexed reduced ferrocenecarboxylic acid
$\beta$ -CD/Fp-PVBC	$\beta$ -Cyclodextrin-complexed poly(cyclopentadienylvinylbenzylidicarbonyliron)
$\beta$ -CD/Fp-VBC	$\beta$ -Cyclodextrin-complexed cyclopentadienylvinylbenzylidicarbonyliron)
$\beta$ -CD/Fp <sub>2</sub>	$\beta$ -Cyclodextrin-complexed cyclopentadienyl dicarbonyl iron dimer
Cp	Cyclopentadienyl
CV	Cyclic voltammetry
DDAT	S-1-Dodecyl-S'-(a,a'-dimethyl-a''-acetic acid) trithiocarbonate
DMF	Dimethylformamide
Fc	Ferrocene

FCA <sup>-</sup>	Reduced ferrocenecarboxylic acid
Fp	Cyclopentadienyl dicarbonyl iron
Fp <sub>2</sub>	Cyclopentadienyl dicarbonyl iron dimer
FpK	Cyclopentadienyldicarbonyliron potassium
FpP	Cyclopentadienyl(dicarbonyl)(diphenylphosphinopropyl)iron
Fp-VBC	Cyclopentadienylvinylbenzyldicarbonyliron
Fp-PVBC	Poly(cyclopentadienylvinylbenzyldicarbonyliron)
FTIR	Fourier transform infrared
GPC	Gel permeation chromatography
HMDI	Hexamethylene diisocyanate
HMQC	Heteronuclear multiple quantum coherence
MC	Metal carbonyl
MCP	Metal-containing polymer
MIP	Migration insertion polymerization
MIR	Migration insertion reaction

$M_n$	Number-average molecular weight
$M_w$	Weight-average molecular weight
NMR	Nuclear magnetic resonance
NG	Nitroglycerin
PEG	Poly(ethylene glycol)
PDI	Polydispersity index
PFpP	Poly(cyclopentadienyldicarbonyldiphenylphosphinopropyliron)
PS- <i>b</i> -PPES	Polystyrene-block-poly((4-phenylethynyl) styrene)
PVBC	Poly(vinylbenzyl chloride)
PVFc	Poly(vinylferrocene)
RAFT	Radical addition-fragmentation chain transfer
ROP	Ring-opening polymerization
ROMP	Ring-opening metathesis polymerization
SLS	Static light scattering
TGA	Thermogravimetric analysis

THF	Tetrahydrofuran
VBC	Vinylbenzyl chloride
VFc	Vinylferrocene
UV	Ultraviolet
UV-Vis	Ultraviolet–visible spectroscopy

## **1. Introduction**

### **1.1 Metal-containing polymers**

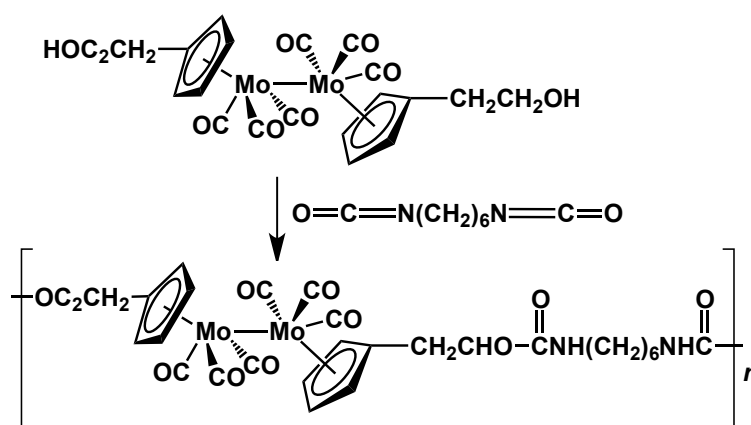
Metal-containing polymers (MCPs) have attracted considerable attention in materials science, because they display many interesting properties, *e.g.*, luminescence, conductivity and magnetism.<sup>[1-5]</sup> However, only a few MCPs, *e.g.*, polymetallocenes,<sup>[6]</sup> coordination polymers,<sup>[7]</sup> are stable enough to allow possible material processing.

Metal carbonyl (MC) polymers, a group of macromolecules containing MC complexes, are usually unstable and undergo decomposition or cross-linking during the synthesis.<sup>[8-9]</sup> Despite the difficulties in synthesis,<sup>[9-11]</sup> a number of MC polymers have been prepared during the past decades,<sup>[2,8,10,12-13]</sup> and some of them have been developed into functional materials.<sup>[2-3,12]</sup> The synthesis of these MC polymers is briefly summarized below.

#### **1.1.1 Main-chain MC polymers**

Main-chain MC polymers can be prepared using a number of well-developed polymerization techniques including step-growth polymerization,<sup>[14]</sup> ring-opening

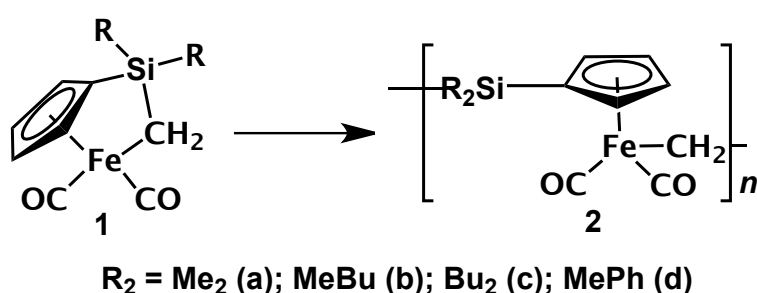
metathesis polymerization (ROMP)<sup>[11]</sup> and thermal ring-opening polymerization (ROP).<sup>[10]</sup> As shown in **Scheme 1**, the bifunctional molybdenum (Mo) carbonyl complex,  $(\eta^5\text{-C}_5\text{H}_4)_2\text{Mo}_2(\text{CO})_6$ , undergoes step-growth polymerization with hexamethylene diisocyanate (HMDI), producing a MC polymer with Mo-Mo bonds in the main-chain.<sup>[15]</sup> The obtained MC polymer is light-labile and degradable *via* metal-metal homolysis when exposed to ultraviolet (UV) radiation.<sup>[15-16]</sup>



**Scheme 1.** Synthesis of main-chain MC polymers *via* step-growth polymerization.<sup>[15]</sup>

As shown in **Scheme 2**, the main-chain MC polymers **2 (a, b, d)** containing Si elements in the backbone were produced *via* ROP of corresponding ring-strained complexes **1 (a, b, d)**. However, during the purification, polymer **2(d)** became insoluble after it was precipitated into *n*-hexane. The freshly prepared polymers **2(a)**

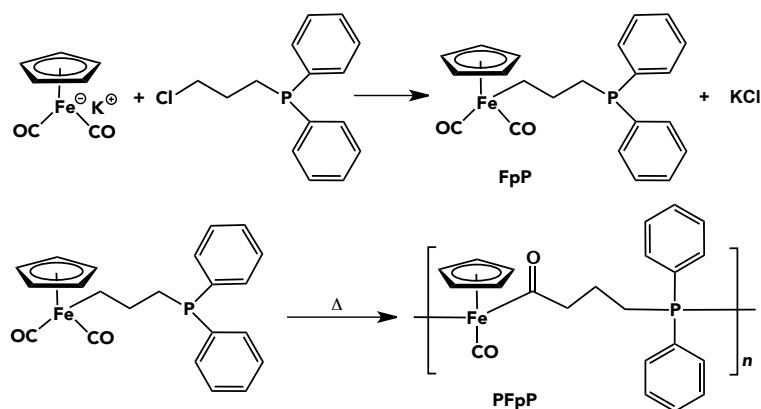
and **2(b)** were soluble in THF, but their solubility decreased when stored in air over a period of time, presumably due to the occurrence of cross-linking.<sup>[10]</sup> Thermal, anionic and transition-metal-catalyzed ROPs of di-*n*-butyl complex **1(c)** have been attempted, but were all unsuccessful.<sup>[10]</sup>



**Scheme 2.** Synthesis of main-chain MC polymers *via* ROP.<sup>[10]</sup>

A new polymerization technique, migration insertion polymerization (MIP), has been developed for the synthesis of air-stable main-chain MC polymers.<sup>[17]</sup> As shown in **Scheme 3**, cyclopentadienyl(dicarbonyl)(diphenylphosphinopropyl)iron (FpP), with the functional group dicarbonylcyclopentadienyliron (Fp) tethered with a phosphine (P) was prepared *via* the reaction of 1-chlorodiphenylphosphinopropane with cyclopentadienyldicarbonyliron potassium (FpK). At elevated temperature, FpP underwent intermolecular migration insertion reactions (MIR), followed by

step-growth polymerization, producing the air-stable MC polymer (PFpP).<sup>[17]</sup>

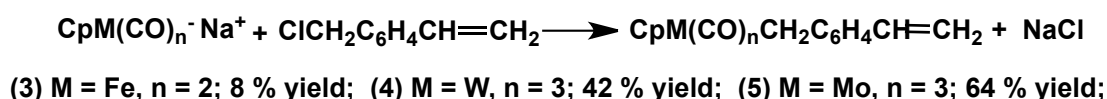


**Scheme 3.** Synthesis of main-chain MC polymers *via* MIP.<sup>[17]</sup>

### 1.1.2 Side-chain MC polymers

Side-chain MC polymers can be synthesized *via* direct polymerization of MC monomers using a number of techniques including free radical polymerization,<sup>[18-19]</sup> step-growth polymerization<sup>[20-21]</sup> and ROMP.<sup>[2]</sup> As shown in **Scheme 4**, transition metal vinylbenzyls can be prepared by the reaction of metal anions with vinylbenzyl chloride (VBC).<sup>[9]</sup> The iron complex **3** was obtained in a low yield because of its instability in solution and difficulties in the purification. The tungsten (W) complex **4** and molybdenum (Mo) complex **5**, obtained in reasonable quantities, were copolymerized with many organic monomers, *e.g.*, styrene, methyl methacrylate, acrylonitrile, *via* free radical polymerization.<sup>[9]</sup> However, these copolymers were

obtained in low yields and were poorly characterized. The content of these MC complexes in the resulting copolymers was inconsistent with the theoretical values calculated based on the ratios of the MC monomers to organic monomers used in the reaction. For example, the Mo content in the copolymers prepared from styrene and complexes **5** was very low (0.2 wt.%) though the ratio of styrene to complex **5** used was 4:1.<sup>[9]</sup> In another case, the copolymerization of ( $\eta^5$ -cyclopentadienyl)vinylbenzyltricarbonylmanganese and styrene resulted in copolymers with low molecular weights, probably due to the instability of the metal-benzyl bonds.<sup>[22]</sup>

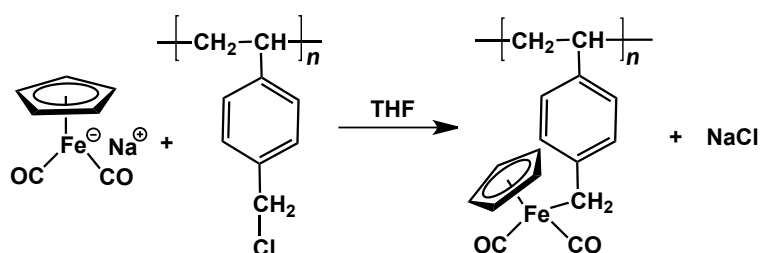


**Scheme 4. Synthesis of transition metal vinylbenzyls *via* substitution reaction.**<sup>[9]</sup>

Side-chain MC polymers can also be synthesized by post-polymerization modification.

As shown in **Scheme 5**, Fp anions react with chloromethylated polystyrene in tetrahydrofuran (THF), producing iron carbonyl polymers. Although the replacement of the chloride groups was complete, the purification was difficult and the resulting

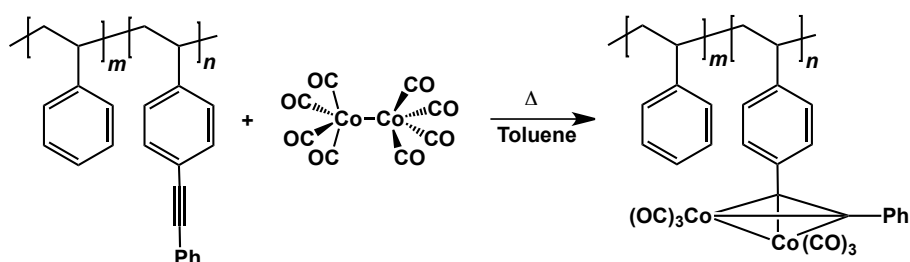
products were cross-linked. When the stoichiometric ratio of Fp anions to phenyl groups was very low (0.15 to 0.30), the resulting polymers were soluble in common organic solvents, *e.g.*, THF, dichloromethane (DCM) and benzene. Similarly, the reaction of Fp anions with partially chloromethylated polystyrene (25 %) also generated soluble polymers. However, the molecular weight distribution of the modified polymers increased, as evidenced by gel permeation chromatography (GPC) analysis.<sup>[23]</sup>



**Scheme 5. Synthesis of side-chain iron carbonyl polymers *via* post-polymerization modification.**<sup>[23]</sup>

As shown in **Scheme 6**, cobalt-containing diblock copolymers have been prepared by mixing polystyrene-*b*-poly((4-phenylethynyl)styrene) (PS-*b*-PPES) and  $\text{Co}_2(\text{CO})_8$  (1 equiv of  $\text{Co}_2(\text{CO})_8$  per PES repeating unit) in toluene at refluxing temperature (*ca.*

110 °C) under N<sub>2</sub>. Elemental analysis revealed that only 80-90 mol% of the alkyne groups reacted with Co<sub>2</sub>(CO)<sub>8</sub> regardless of the reaction time. Heating these polymers in the solid state at 110 °C led to the loss of CO ligands and formation of insoluble cobalt composites. However, when the stoichiometric ratio of Co<sub>2</sub>(CO)<sub>8</sub> to alkyne groups was 1:2, the resulting materials were not soluble in DCM nor toluene, which was attributed to the occurrence of cross-linking.<sup>[8]</sup>



**Scheme 6. Synthesis of side-chain cobalt carbonyl polymers *via* post-polymerization modification.**<sup>[8]</sup>

## 1.2 Cyclodextrin host-guest chemistry

### 1.2.1 Cyclodextrins

Cyclodextrins (CDs) are cyclic oligomers of  $\alpha$ -D-glucopyranose consisting of six ( $\alpha$ -CD), seven ( $\beta$ -CD) or eight ( $\gamma$ -CD) units (**Figure 1**). These CD molecules are water-soluble because all the hydroxyl groups are located at the surface, while their internal cavities are relatively hydrophobic allowing lipophilic molecules with a suitable size to be included *via* host-guest interaction (**Scheme 7**).<sup>[24-25]</sup> The host-guest interaction of CDs derives from van der Waals forces, hydrophobic interactions, hydrogen bonds, along with the influence of electronic effects and steric factors.<sup>[25-26]</sup>  $\alpha$ -CDs are prone to forming stable supramolecular complexes with monocyclic aromatics including azobenzene and its derivatives;  $\beta$ -CDs tend to interact with anthraquinone, cholesterol, ferrocene (Fc), adamantane (Ada) and their derivatives;  $\gamma$ -CDs are apt to form inclusion compounds with larger guest molecules such as pyrene, anthracene and phenanthrene.<sup>[25]</sup>

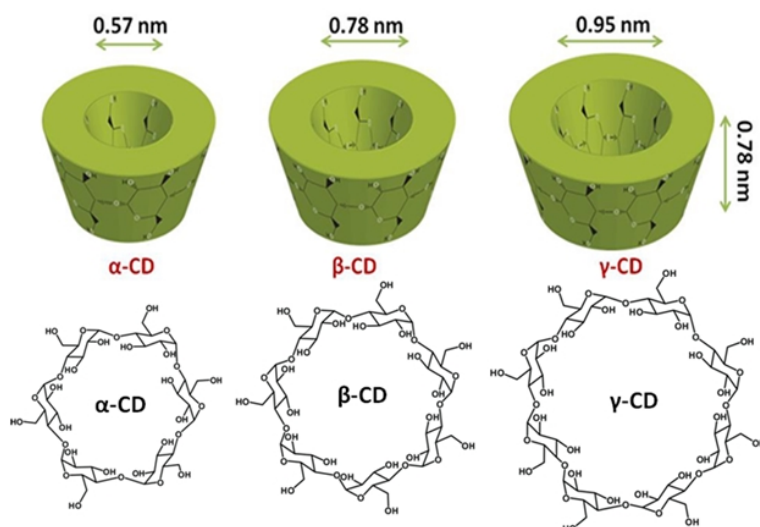
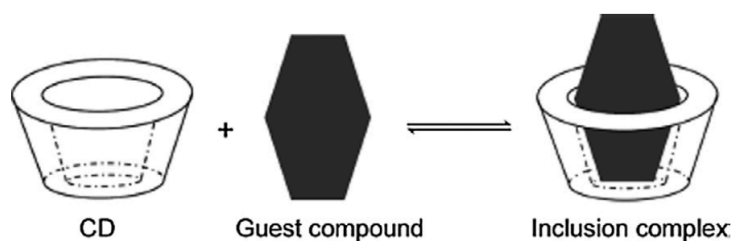


Figure 1. Chemical structures of  $\alpha$ -CD,  $\beta$ -CD and  $\gamma$ -CD.<sup>[24]</sup>



Scheme 7. A schematic representation of the inclusion complex formation between CDs and guest molecules (1:1).<sup>[25]</sup>

The association and dissociation constants determine the stability of the inclusion compounds.<sup>[25,27-29]</sup> For example, the association constant for reduced ferrocenecarboxylic acid ( $\text{FCA}^-$ ) and  $\beta$ -CDs is  $2200 \text{ M}^{-1}$  and their dissociation

constant is less than  $20 \text{ M}^{-1}$  at  $20 \text{ }^\circ\text{C}$ , so  $\text{FCA}^-$  and  $\beta$ -CDs can form stable inclusion compounds ( $\beta$ -CD/ $\text{FCA}^-$ ).<sup>[29]</sup> The association constant for the inclusion compounds can be improved by matching the size of the host and guest molecules. The diameter of the cage-like Ada is approximately  $7 \text{ \AA}$  and its volume is about  $180 \text{ \AA}^3$ , which is close to the hydrophobic cavity of  $\beta$ -CD ( $d = 7 \text{ \AA}$ ,  $v = 270 \text{ \AA}^3$ ). Therefore, Ada can form very stable inclusion compounds with  $\beta$ -CDs. The  $\beta$ -CD complexed Ada has a very high association constant ( $K = 4 \times 10^5 \text{ M}^{-1}$ ), that is higher than that for  $\beta$ -CD/ $\text{FCA}^-$ .<sup>[25,30]</sup> Therefore, Ada derivatives are often used as competitive guest molecules to release Fc-type guest molecules from the internal cavities of  $\beta$ -CDs.<sup>[27-28]</sup>

Upon the formation of CD inclusion compounds, the stability of guest molecules can be significantly improved.<sup>[31-32]</sup> For example, compared with pure vitamin  $\text{D}_3$ , the CD-complexed vitamin  $\text{D}_3$  has higher thermal stability, lower light sensitivity and lower oxygen uptake.<sup>[32]</sup> Nitroglycerin (NG) is an explosive liquid but a useful medicine for heart diseases. After inclusion within  $\beta$ -CDs, NG can be easily made into tablets and is no longer explosive.<sup>[32]</sup>

CD inclusion has also been used to modify the solubility of guest molecules.<sup>[31, 33-34]</sup>

The solubility of guest molecule such as fatty acid, increases linearly with the amount of CDs added.<sup>[33]</sup> Compared with the guest molecules in the free state, their CD inclusion compounds can be dissolved in water more easily and rapidly. Some CD-complexed medicines, even if they are not completely soluble in water, can be finely dispersed in water and can be efficiently absorbed by living organisms.<sup>[34]</sup>

It is also reported that CD inclusion compounds can dramatically increase the fluorescence intensity of dansyl derivatives. When these CD-complexed dansyl derivatives are employed in peptide analysis, the detection limit can be improved significantly.<sup>[35]</sup>

### **1.2.2 CD inclusion compounds of metal complexes**

CD inclusion compounds of metal complexes have been explored for decades.<sup>[25-26,28,36-47]</sup> For example, the molecular mobility of  $(\eta^5\text{-C}_5\text{H}_5)\text{Fe}(\text{CO})_2\text{I}$  and its  $\beta$ -CD inclusion compounds was investigated using solid-state nuclear magnetic

resonance (NMR) spectroscopy. In its free state, the rotation of the cyclopentadienyl (Cp) ring is fast but the two CO groups are static because of crystal-packing constraints. Upon the formation of inclusion compounds with  $\beta$ -CDs, its overall molecular mobility is increased and the CO groups, previously reported to be static, also gain mobility.<sup>[36]</sup>

The thermal stability of  $\text{Mn}_2(\text{CO})_{10}$  and its  $\gamma$ -CD inclusion compounds was revealed by thermogravimetric analysis (TGA) that was performed under argon. As shown in **Figure 2**, a mixture of free  $\text{Mn}_2(\text{CO})_{10}$  and  $\gamma$ -CDs shows two stages of weight-loss, representing the decomposition temperatures of the two components.  $\gamma$ -CDs decompose at *ca.* 300 °C and  $\text{Mn}_2(\text{CO})_{10}$  decomposes at *ca.* 128 °C. The  $\gamma$ -CD inclusion compounds of  $\text{Mn}_2(\text{CO})_{10}$  are stable up to 174 °C. This enhancement in thermal stability was also confirmed by Fourier transform infrared (FTIR) spectroscopy.  $\text{Mn}_2(\text{CO})_{10}$  and its  $\gamma$ -CD inclusion compounds were separately heated to 140 °C, and these thermally treated samples were collected for FTIR analysis. The spectrum for thermally treated  $\gamma$ -CD-complexed  $\text{Mn}_2(\text{CO})_{10}$  showed strong absorption

peaks due to the CO groups, whereas no CO absorption peaks were observed in the spectrum for thermally treated  $\text{Mn}_2(\text{CO})_{10}$ .<sup>[38]</sup>

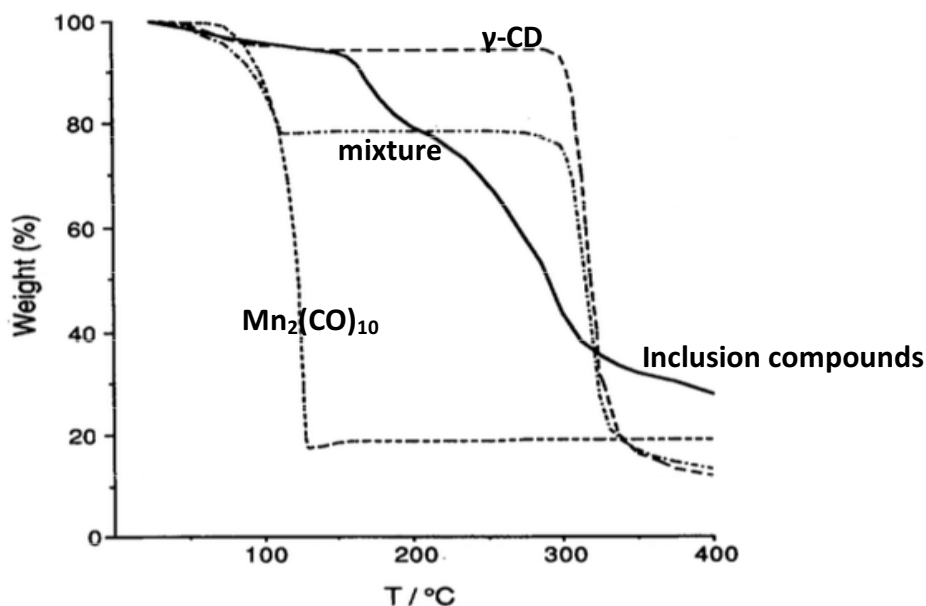
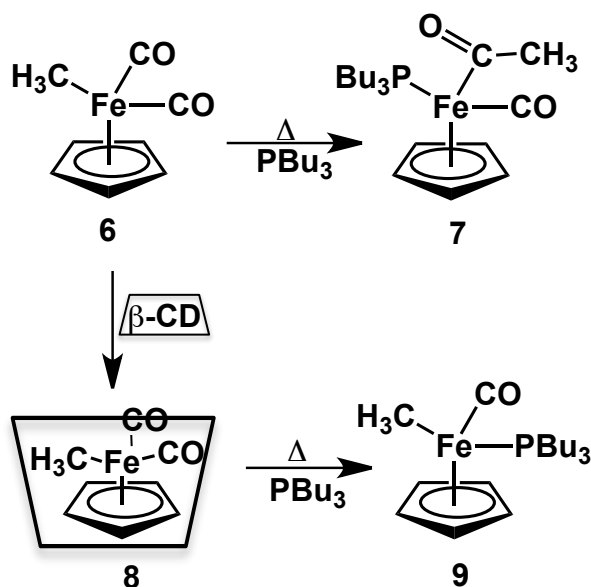


Figure 2. TGA curves for  $\text{Mn}_2(\text{CO})_{10}$  (----), its 1:1  $\gamma\text{-CD}$  inclusion compounds (—),  $\gamma\text{-CD}$  (— · —) and 1:1 mixture of  $\text{Mn}_2(\text{CO})_{10}$  and  $\gamma\text{-CD}$  (— · · —).<sup>[38]</sup>

As shown in **Scheme 7**,  $[(\eta^5\text{-C}_5\text{H}_5)\text{Fe}(\text{CO})_2(\text{CH}_3)]$  (complex **6**) participates in a CO migration insertion reaction (MIR) producing complex **7** when it is heated in the presence of phosphines,<sup>[26]</sup> whereas its  $\beta\text{-CD}$  inclusion compound **8** undergoes a ligand substitution reaction producing complex **9** under the same condition. Therefore, CD inclusion can drastically influence the thermal reaction of

$[(\eta^5\text{-C}_5\text{H}_5)\text{Fe}(\text{CO})_2(\text{CH}_3)]$  with phosphines. The ligand substitution reaction of complex **8** is probably caused by steric hindrance between  $\beta$ -CDs and the ligands, which slows down the rate of the alkyl migration reaction. Upon substitution, complex **9** is released from the cavity of  $\beta$ -CD, which is also attributed to steric effects.<sup>[26,39]</sup>



**Scheme 8.** Schematic illustration for the MIR of MC complexes (**6**) with phosphines and the ligand substitution reaction of  $\beta$ -CD-complexed MC (**8**) with phosphines.<sup>[39]</sup>

### 1.2.3 Polymer inclusion complexes with CDs

Polymers can also interact with CDs for the formation of inclusion complexes.

CD-complexed polymers can be divided into two types: main-chain CD-complexed

polymers and side-chain CD-complexed polymers.<sup>[48]</sup> For example,  $\alpha$ -CDs can form main-chain inclusion complexes with poly(ethylene glycol) (PEG). The structure of  $\alpha$ -CD complexed PEG was confirmed by single crystal X-ray crystallography (**Figure 3**). The PEG chain was included in the channel formed by a stack of  $\alpha$ -CDs.<sup>[49]</sup>

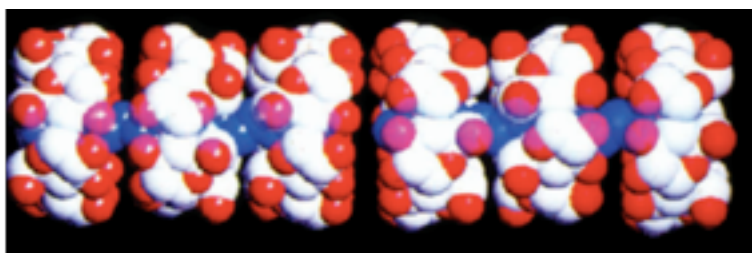


**Figure 3.** The crystal structure for  $\alpha$ -CD complexed PEG.<sup>[49]</sup>

As shown in **Figure 4**, complexation of the Ada side-groups on adamantyl polyphosphazene-*b*-polystyrene copolymers (APN-*b*-PS) with  $\beta$ -CDs was attempted in aqueous solution. APN-*b*-PS was insoluble in water. However, after the addition of  $\beta$ -CD, the solution became clear and the formation of micelles was detected by dynamic light scattering (DLS). This observation suggested that the hydrophobic diblock copolymers were modified to amphiphilic polymers ( $\beta$ -CD/APN-*b*-PS) *via* host-guest interactions of  $\beta$ -CDs with the Ada units. The resulting amphiphilic

polymers self-assembled into micelles with PS blocks as the core and  $\beta$ -CD/APN blocks as the shell. The formation of the micelles could be controlled by varying the ratio of  $\beta$ -CDs to Ada units on the polymers. A critical ratio of  $\beta$ -CD to Ada groups was needed to provide enough hydrophilicity for the formation of micelles, which was determined using pyrene as a fluorescence probe. Pyrene is expected to be partitioned into the hydrophobic PS core of the micelles, resulting in an enhancement in the excitation intensity of pyrene.<sup>[50]</sup> This enhancement was observed when the ratio of  $\beta$ -CD to Ada groups was greater than 0.4. Therefore, the critical ratio of  $\beta$ -CDs to Ada groups for micellization was 0.4.<sup>[51]</sup>

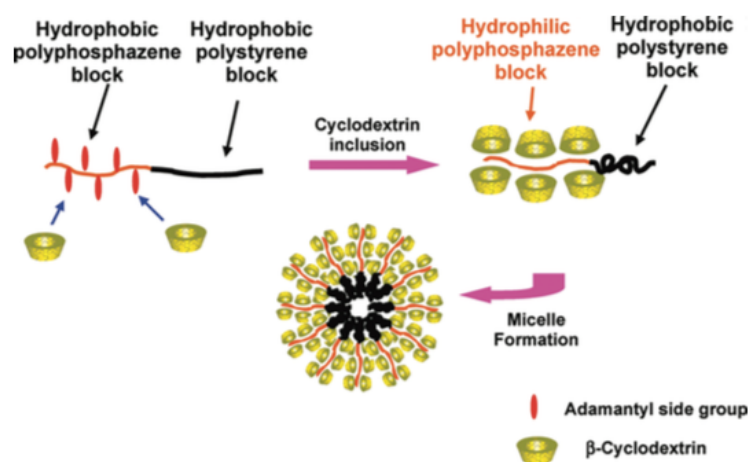
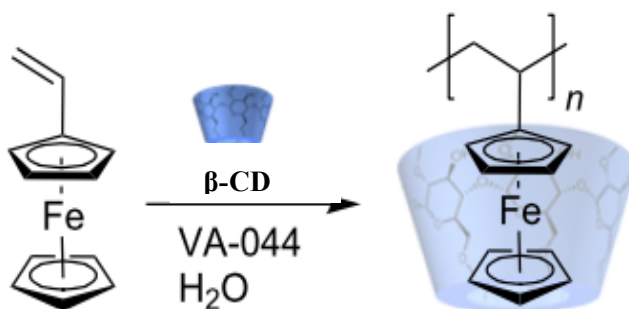


**Figure 4. Synthesis of  $\beta$ -CD complexed APN-*b*-PS diblock copolymers and micelle formation.**<sup>[51]</sup>

As shown in **Scheme 9**, the direct polymerization of CD-complexed vinyl monomers was attempted. Although vinylferrocene (VFc) is hydrophobic,  $\beta$ -CD-complexed VFc could be polymerized in water at 50 °C *via* free radical polymerization using VA-044 as initiator. During polymerization, the viscosity of the solution increased due to the formation of polymer, but no precipitate was observed because the  $\beta$ -CD-complexed PVFc was hydrophilic. After stirring for 48 h, the reaction solution was freeze-dried and no residual monomer was evidenced by thin layer chromatography. Upon heating the resulting  $\beta$ -CD-complexed PVFc in a hydrogen peroxide solution, the color of this solution changed from yellow (**Figure 5a**) to green (**Figure 5b**). In this step, hydrophobic PVFc was oxidized to hydrophilic PVFc<sup>+</sup>, resulting in the release of PVFc<sup>+</sup> from the hydrophobic cavities of  $\beta$ -CDs. Over a period of time, an orange precipitate was observed (**Figure 5c**), which was probably due to the reduction of PVFc<sup>+</sup> back to PVFc. However, the orange precipitate was not characterized to explain the proposed reduction process. In another example, when potassium 1-adamantane carboxylate was added as a competitive guest molecule to an aqueous

solution of  $\beta$ -CD complexed PVFc, a precipitate was observed due to the release of the hydrophobic uncomplexed PVFc from the cavities of  $\beta$ -CDs.<sup>[28]</sup>



**Scheme 9. Free radical polymerization of VFc in the presence of  $\beta$ -CDs using VA-044 as initiator.**<sup>[28]</sup>

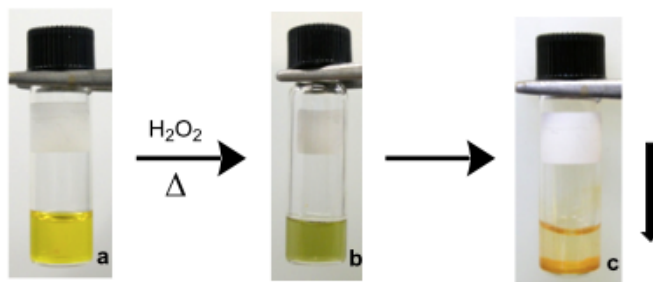


**Figure 5. Aqueous solution of  $\beta$ -CD-complexed PVFc (a) was mixed with hydrogen peroxide and heated to 50 °C (b); orange precipitate observed (c).**<sup>[28]</sup>

Because CD can complex with organometallic molecules to produce air-stable inclusion compounds and this host-guest chemistry also works for polymers, we propose to synthesize CD-complexed MC polymers. This work addresses the challenge encountered in the synthesis of air-stable MC polymers.

## 2. Experimental procedures

### Materials

Sodium (Na), potassium (K), VBC, cyclopentadienyliron dicarbonyl dimer (Fp<sub>2</sub>), β-CD, 1-dodecanethiol, chloroform, tricaprylylmethylammonium chloride (Aliquat 336), carbon disulfide (CS<sub>2</sub>), benzophenone, azobisisobutyronitrile (AIBN) and sodium hydroxide (NaOH) were purchased from Sigma-Aldrich. All the experiments were performed under N<sub>2</sub> using standard Schlenk techniques. THF was freshly distilled under N<sub>2</sub> from Na/benzophenone. *n*-Hexane, toluene, acetone, dimethyl sulfoxide (DMSO) and DCM were degassed with N<sub>2</sub> before use. AIBN was purified by three repeated recrystallizations from ethanol. VBC was passed through a neutral alumina column to remove inhibitors before the polymerization. Other chemicals were used as received unless otherwise indicated.

## Instrumentation

$^1\text{H}$  NMR spectra,  $^{13}\text{C}$  NMR spectra and  $^1\text{H}$ - $^{13}\text{C}$  heteronuclear multiple quantum coherence (HMQC) 2D NMR spectra were obtained on a Bruker Avance 300 spectrometer at ambient temperature using appropriate deuterated solvents. The  $^1\text{H}$  chemical shifts were referenced to the solvent peak DMSO (2.49 ppm),  $\text{CHCl}_3$  (7.24 ppm) and the  $^{13}\text{C}$  chemical shifts were referenced to the solvent peak DMSO (39.5 ppm).

Gel permeation chromatography (GPC) was used to characterize the molecular weights and molecular weight distributions of the polymers at room temperature. THF was used as eluent at a flow rate of 1.0 mL/min on a system equipped with three PlolyAnalytik mixed bed columns, PAS-103-L, PAS-104-L and PAS-105-L, each with dimensions of 8 mm (i.d.)  $\times$  300 mm (L), and a Viscotek triple detector array including refractive index, viscosity and dual-angle light scattering detectors. Polystyrene standards were used as references.

Fourier transform infrared (FTIR) spectra for solid samples were recorded on a Bruker Tensor 27 spectrophotometer. All the samples were dried at 40 °C under vacuum overnight. Test pellets were prepared by grinding and compressing the solids products in KBr.

Thermal gravimetric analysis (TGA) was performed on a TGA Q500 at a heating rate of 10 °C/min under N<sub>2</sub> flow. The samples were dried at 40 °C under vacuum overnight before the measurement.

Cyclic voltammetry (CV) was performed using a CHI604 electrochemical workstation equipped with a Ag reference electrode. The samples (5 mg) were dissolved in 10 mL DMSO containing 10 mg tetrabutylammonium perchlorate (TBAP). The potential scan rate was 100 mVs<sup>-1</sup>.

## 2.1 Synthesis of poly(vinyl benzyl chloride) (PVBC)

### 2.1.1 Synthesis of S-1-dodecyl-S'-(a,a'-dimethyl-a'')-acetic acid trithiocarbonate (DDAT)

DDAT was prepared according to the literature.<sup>[52]</sup> 1-Dodecanethiol (4.04 g, 20.00 mmol), acetone (9.62 g, 0.17 mol) and Aliquat 336 (0.32 g, 0.80 mmol) were mixed in a Schlenk flask. A NaOH solution (50 wt.%) (1.67 g, 21.00 mmol) was added dropwise to the flask over 20 min. After 15 min, CS<sub>2</sub> (1.52 g, 20.00 mmol) in acetone (2.02 g, 34.50 mmol) was added dropwise to the flask over 20 min. After the solution was stirred for another 10 min, chloroform (3.56 g, 30.00 mmol) was added in one portion, followed by the drop-wise addition of a NaOH solution (50 wt.%) (8.00 g, 0.10 mol) over 30 min. The reaction was then stirred overnight. On the second day, 30.0 mL of water were added to the solution, followed by 5.0 mL of concentrated HCl. The flask was purged with N<sub>2</sub> to evaporate off the acetone. The resulting solids were collected by filtration and then dissolved in 50.0 mL 2-propanol. After removing undissolved solids, the 2-propanol solution was concentrated and recrystallized from *n*-hexane to produce a yellow solid. Yield: 3.79 g, 52 %. <sup>1</sup>H NMR (CDCl<sub>3</sub>): 0.86 ppm

(3H, -CH<sub>3</sub>), 1.23–1.32 ppm (18H, -CH<sub>2</sub>CH<sub>2</sub>(CH<sub>2</sub>)<sub>9</sub>CH<sub>3</sub>), 1.56–1.62 ppm [(2H, -CH<sub>2</sub>C<sub>10</sub>H<sub>21</sub>) and (s, 6H, -C(CH<sub>3</sub>)<sub>2</sub>COOH)], 3.26 ppm (2H, -S-CH<sub>2</sub>C<sub>11</sub>H<sub>23</sub>).

### 2.1.2 RAFT homopolymerization of VBC using DDAT

DDAT (0.25 g, 0.68 mmol), VBC (7.78 g, 51.00 mmol), AIBN (0.03 g, 0.17 mmol) and toluene (40.0 mL) were placed in a dry Schlenk flask with a magnetic stir bar.

After degassing with N<sub>2</sub> at 23 °C for 30 min, the solution was stirred at 75 °C for 24 h.

The reaction was terminated by rapidly cooling the flask in an ice bath. The polymerization solution was precipitated into excess methanol (*ca.* 500 mL). The

yellow precipitate obtained in methanol was collected and dried under vacuum overnight. Yield: 3.88 g, 48 %. <sup>1</sup>H NMR (CDCl<sub>3</sub>): 0.86 (3H, -CH<sub>3</sub>), 4.51 ppm (2H,

-C<sub>6</sub>H<sub>4</sub>-CH<sub>2</sub>-Cl), 6.47-7.06 ppm (4H, -C<sub>6</sub>H<sub>4</sub>-CH<sub>2</sub>-Cl), 3.25 ppm (2H, -S-CH<sub>2</sub>C<sub>11</sub>H<sub>23</sub>),

1.24-1.67 ppm (protons from the polymer backbone, -CH<sub>2</sub>-CH-). <sup>13</sup>C NMR

(DMSO-*d*<sub>6</sub>): 134.75 ppm; 128.54 ppm; 127.47 ppm; 145.08 ppm (-C<sub>6</sub>H<sub>4</sub>-CH<sub>2</sub>-Cl),

46.11 ppm (-C<sub>6</sub>H<sub>4</sub>-CH<sub>2</sub>-Cl), 22.36-31.36 ppm (carbons from the polymer backbone,

-CH<sub>2</sub>-CH-). GPC: Number-average molecular weight (M<sub>n</sub>) = 5200 g/mol,

weight-average molecular weight ( $M_w$ ) = 5900 g/mol, polydispersity index (PDI) = 1.13.

## **2.2 Synthesis of cyclopentadienyldicarbonyliron potassium (FpK)**

FpK was synthesized according to a procedure in reported the literature.<sup>[53]</sup> A THF solution (50.0 mL) of benzophenone (9.11 g, 50 mmol) and potassium (1.96 g, 50 mmol) was stirred at room temperature overnight. After Fp<sub>2</sub> (8.85 g, 25 mmol) was added, the color of the THF solution gradually turned from dark blue to reddish and an orange precipitate was formed. After the solution was stirred for 3 h, the THF was removed under vacuum and the orange residue (FpK) was washed with toluene to remove benzophenone and unreacted Fp<sub>2</sub>. FpK was finally dried under vacuum overnight. Yield: 7.02 g, 65 %.

## **2.3 Synthesis of Fp-modified VBC (Fp-VBC)**

VBC (1.55 g, 10.0 mmol) and FpK (2.40 g, 11.0 mmol) were dissolved in THF (30.0 mL) at 23 °C. After stirring for 3 h, the solution was filtered through a plug of Celite

to remove the KCl formed. The reddish brown filtrate was collected and concentrated to 3-5 mL and purified by chromatography on a silica gel column using *n*-hexane/DCM (9.5:0.5, v/v) as eluent. After removing the solvents under vacuum, a yellow solid was collected. Yield: 2.30 g, 58 %. <sup>1</sup>H NMR (DMSO-*d*<sub>6</sub>): 5.11 ppm, 5.63 ppm, 6.54 ppm (3H, **CH**<sub>2</sub>=**CH**-), 7.03-7.17 ppm (4H, -C<sub>6</sub>**H**<sub>4</sub>-), 2.64 ppm (2H, -C<sub>6</sub>H<sub>4</sub>-**CH**<sub>2</sub>-), 4.93 ppm (5H, C<sub>5</sub>**H**<sub>5</sub>-Fe-), 3.30 ppm (**H**<sub>2</sub>O).

## 2.4 Synthesis of Fp-modified PVBC (Fp-PVBC)

PVBC (M<sub>n</sub> = 5200 g/mol, PDI = 1.13, 1.0 g, 0.20 mmol) was added to a THF (15.0 mL) solution of FpK (1.51 g, 7.00 mmol) at 23 °C. After stirring for 3 h, the solution was passed through a plug of Celite to remove the KCl formed. The reddish-brown filtrate was collected and concentrated to 3-5 mL. The concentrated solution was added to *n*-hexane, yielding a yellow precipitate. The yellow solid was collected by filtration and dried under vacuum at room temperature overnight. Yield: 1.36 g, 54 %. This yellow product was not completely soluble in common organic solvents, *e.g.*, THF, CHCl<sub>3</sub> and DMSO. CDCl<sub>3</sub> solution of the product was centrifuged and the

supernatant was used for  $^1\text{H}$  NMR analysis.  $^1\text{H}$  NMR ( $\text{CDCl}_3$ ): 6.32-6.86 ppm (4H,  $-\text{C}_6\text{H}_4-$ ), 4.45 ppm (5H,  $\text{C}_5\text{H}_5\text{-Fe-}$ ), 2.59 ppm (2H,  $-\text{C}_6\text{H}_4\text{-CH}_2-$ ), 0.86 (3H,  $-\text{CH}_3$ ), 1.24-1.71 ppm (protons from the polymer backbone,  $-\text{CH}_2\text{-CH-}$ ).

## 2.5 Synthesis of $\beta$ -CD-complexed Fp-VBC ( $\beta$ -CD/Fp-VBC)

Fp-VBC (0.44 g, 1.5 mmol) was added to a saturated aqueous solution of  $\beta$ -CD (2.27 g, 2.0 mmol). This solution was stirred vigorously at 40 °C overnight. The resulting yellow precipitate was collected by filtration. The precipitate was washed with water to remove  $\beta$ -CD, and with THF to remove unreacted Fp-VBC. The yellow solid was collected by filtration and then dried under vacuum. Yield: 1.45 g, 54 %.  $^1\text{H}$  NMR ( $\text{DMSO-}d_6$ ): 7.03-7.17 ppm (4H,  $-\text{C}_6\text{H}_4-$ ), 6.54 ppm, 5.63 ppm, 5.11 ppm (3H,  $\text{CH}_2=\text{CH-}$ ), 2.64 ppm (2H,  $-\text{C}_6\text{H}_4\text{-CH}_2-$ ), 4.93 ppm (5H,  $\text{C}_5\text{H}_5\text{-Fe-}$ ), 5.66-5.72 ppm (14H,  $\text{C}_{2,3}\text{-OH-(CD)}$ ), 4.82 ppm (7H,  $\text{C}_1\text{-H-(CD)}$ ), 4.43 ppm (7H,  $\text{C}_6\text{-H-(CD)}$ ), 3.63 ppm (21H,  $\text{C}_{3,5,6}\text{-H-(CD)}$ ), 3.3 ppm (14H,  $\text{C}_{2,4}\text{-H-(CD)}$ ).  $^{13}\text{C}$  NMR ( $\text{DMSO-}d_6$ ): 136.82 ppm, 131.70 ppm, 127.14 ppm, 125.83 ppm ( $-\text{C}_6\text{H}_4-$ ), 86.50 ppm ( $\text{C}_5\text{H}_5\text{-Fe-}$ ), 101.94 ppm ( $\text{C}_1\text{-H-(CD)}$ ), 81.53 ppm ( $\text{C}_4\text{-H-(CD)}$ ), 73.04 ppm, 72.41 ppm, 72.03

ppm ( $C_{2,3,5}$ -H-(CD)), 59.90 ppm ( $C_6$ -H-(CD)), 4.23 ppm ( $-C_6H_4-CH_2-$ ), 111.60 ppm, 153.43 ppm ( $CH_2=CH-$ ), 217.62 ppm (CO-Fe-).

## 2.6 Synthesis of $\beta$ -CD-complexed Fp-PVBC ( $\beta$ -CD/Fp-PVBC)

PVBC ( $M_n = 5200$  g/mol, 0.5 g, 0.10 mmol) was added to a THF (15.0 mL) solution of FpK (0.756 g, 3.50 mmol) at room temperature. After stirring for 3 h, the solution was filtered through a plug of Celite to remove the KCl formed. The reddish-brown filtrate was collected and concentrated to approximately 3-5 mL. An aqueous solution (40 °C) of  $\beta$ -CD (3.75 g, 3.3 mmol) in water (120 mL) was then added drop-wise to the concentrated solution, generating a large quantity of precipitate. The color of the precipitate gradually turned from yellow to reddish during the complexation with  $\beta$ -CD. The turbid solution was then vigorously stirred at 40 °C for 24 h. The resulting reddish precipitate was collected by filtration and washed with water to remove uncomplexed  $\beta$ -CD, and with THF to remove uncomplexed Fp-PVBC. After drying under vacuum overnight, the reddish solid was dissolved in a small amount of DMSO. Upon removal of the undissolved material by centrifugation, the transparent DMSO

solution was precipitated into excess water, resulting in an reddish precipitate. The final product was collected by filtration and then dried under vacuum. Yield: 2.20 g, 45 %.  $^1\text{H}$  NMR (DMSO- $d_6$ ): 7.17-7.24 ppm (4H,  $-\text{C}_6\text{H}_4-$ ), 4.99 ppm (5H,  $\text{C}_5\text{H}_5\text{-Fe-}$ ), 2.29 ppm (2H,  $-\text{C}_6\text{H}_4\text{-CH}_2-$ ), 1.23-1.75 ppm (protons from the polymer backbone,  $-\text{CH}_2\text{-CH-}$ ), 5.66-5.72 ppm (14H,  $\text{C}_{2,3}\text{-OH-(CD)}$ ), 4.82 ppm (7H,  $\text{C}_1\text{-H-(CD)}$ ), 4.43 ppm (7H,  $\text{C}_6\text{-H-(CD)}$ ), 3.63 ppm (21H,  $\text{C}_{3,5,6}\text{-H-(CD)}$ ), 3.3 ppm (14H,  $\text{C}_{2,4}\text{-H-(CD)}$ ).  $^{13}\text{C}$  NMR (DMSO- $d_6$ ): 137.35 ppm, 128.88 ppm, 128.20 ppm, 125.32 ppm ( $-\text{C}_6\text{H}_4-$ ), 88.59 ppm ( $\text{C}_5\text{H}_5\text{-Fe-}$ ), 101.94 ppm ( $\text{C}_1\text{-H-(CD)}$ ), 81.55 ppm ( $\text{C}_4\text{-H-(CD)}$ ), 73.04 ppm, 72.41 ppm, 72.03 ppm ( $\text{C}_{2,3,5}\text{-H-(CD)}$ ), 59.91 ppm ( $\text{C}_6\text{-H-(CD)}$ ), 21.07 ppm ( $-\text{C}_6\text{H}_4\text{-CH}_2-$ ).

## 2.7 Synthesis of CD-complexed $\text{Fp}_2$ ( $\beta\text{-CD/Fp}_2$ )

$\text{Fp}_2$  (0.20 g, 0.57 mmol) was added to a saturated aqueous solution (40 °C) of  $\beta\text{-CD}$  (1.4 g, 1.2 mmol) in water (50 mL). This solution was stirred vigorously at 40 °C overnight. The resulting reddish precipitate was collected by filtration and then washed with water to remove uncomplexed  $\beta\text{-CD}$ , and with toluene to remove

uncomplexed  $\text{Fp}_2$ . The reddish solid was dissolved in a small amount of DMSO. After the undissolved material in DMSO was removed by filtration, the transparent DMSO solution was precipitated into excess water, producing a reddish precipitate. The final product was collected by filtration and then dried under vacuum. Yield: 1.10 g, 68 %.

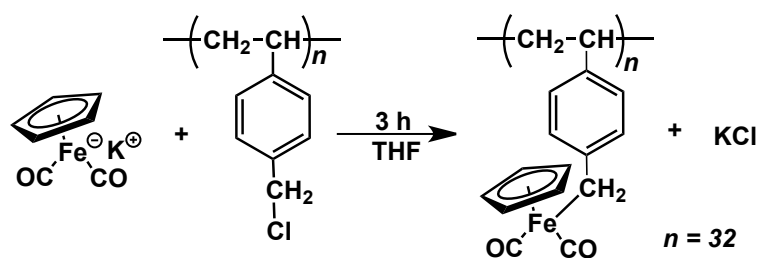
$^1\text{H}$  NMR ( $\text{DMSO-}d_6$ ): 4.99 ppm (5H,  $\text{C}_5\text{H}_5\text{-Fe-}$ ), 5.66-5.72 ppm (14H,  $\text{C}_{2,3}\text{-OH-(CD)}$ ), 4.82 ppm (7H,  $\text{C}_1\text{-H-(CD)}$ ), 4.43 ppm (7H,  $\text{C}_6\text{-H-(CD)}$ ), 3.63 ppm (21H,  $\text{C}_{3,5,6}\text{-H-(CD)}$ ), 3.3 ppm (14H,  $\text{C}_{2,4}\text{-H-(CD)}$ ).

### 3. Results and discussion

#### 3.1 Synthesis of Fp-PVBC

We first attempted to synthesize Fp-PVBC *via* post-polymerization modification of PVBC using Fp anions in THF (**Scheme 10**). No insoluble material was generated during the reaction. After the reaction, the solution was passed through a plug of Celite to remove salts and was then concentrated. The concentrated solution was precipitated into *n*-hexane in air, resulting in a yellow precipitate. We found that the precipitated product was not completely soluble in organic solvents, *e.g.*, THF, toluene, DMSO. When the yellow product was dissolved in THF, a large quantity (more than 50 wt.%) of dark yellow insoluble material was generated. A similar observation was reported before for the reaction of linear chloromethylated polystyrene with Fp anions, resulting in a cross-linked polymer.<sup>[23]</sup> To test whether the cross-linking was caused by air-instability of the Fp groups, we precipitated the solution of Fp-PVBC into *n*-hexane under N<sub>2</sub> atmosphere, which however could not avoid the generation of insoluble material. The soluble fraction of Fp-PVBC in THF was separated from the dark yellow precipitate by filtration, and then precipitated into

*n*-hexane again. A few cycles of this purification process were performed under N<sub>2</sub> atmosphere, but each cycle generated large quantities of insoluble material. This observation suggested that the cross-linked materials were produced during the precipitation.



**Scheme 10.** Synthesis of Fp-PVBC *via* the post-polymerization modification of PVBC using Fp anions.

The precipitated Fp-PVBC, containing a cross-linked fraction, was first characterized using FTIR spectroscopy. As shown in **Figure 6**, the peak at 1265 cm<sup>-1</sup> due to the  $-\text{CH}_2\text{Cl}$  groups on PVBC (**Figure 6a**) disappears after the post-polymerization modification, suggesting that all the chloride groups were substituted by the Fp groups. The appearance of the two new peaks at 2002 cm<sup>-1</sup> and 1944 cm<sup>-1</sup> in **Figure 6b** also supports the success of the reaction.<sup>[54]</sup> These two peaks are diagnostic

absorptions for the symmetric and asymmetric stretching of CO terminal ligands in Fp groups. The cross-linked materials were assumed to be caused by the dimerization of Fp groups *via* CO bridging (**Scheme 11**).<sup>[55]</sup> If it were the case, a characteristic absorption for the bridging CO groups should appear at 1750-1800  $\text{cm}^{-1}$ .<sup>[54]</sup> However, no peaks are observed in this region in **Figure 6b**, which indicates that dimerization cannot be the reason for the cross-linking.

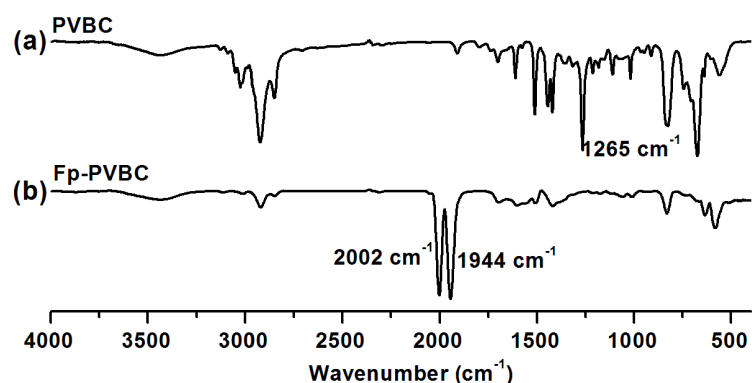
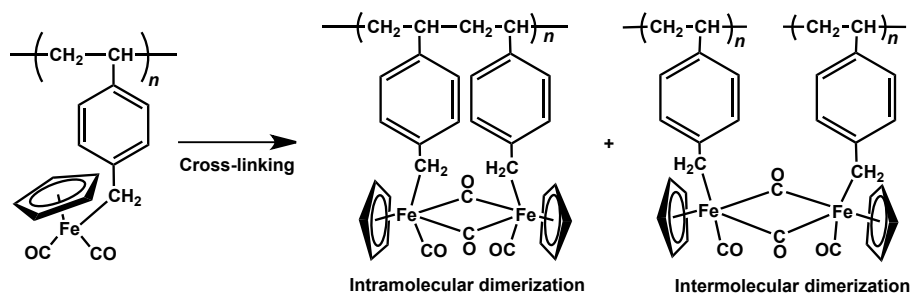


**Figure 6.** FTIR spectra for PVBC (a) and Fp-PVBC (b). note: Fp-PVBC contained cross-linked material.



**Scheme 11.** Possible intramolecular and intermolecular dimerization of Fp-PVBC.

The soluble fraction of Fp-PVBC was characterized by  $^1\text{H}$  NMR spectroscopy. The chemical resonance due to the chloromethyl groups ( $-\text{CH}_2\text{-Cl}$ ) in PVBC at 4.51 ppm (**Figure 7a**) shifts to 2.59 ppm ( $-\text{CH}_2\text{-Fp}$ ) (**Figure 7b**).<sup>[9, 23]</sup> Meanwhile, a signal at 4.55 due to the *Cp* rings in the Fp groups appears in the spectrum (**Figure 7b**), suggesting that the Fp groups were successfully attached to the side-chains of PVBC.<sup>[23]</sup> The integration ratio for the peak due to the *Cp* rings to the peak due to the  $-\text{CH}_2\text{-Fp}$  groups is 2.5:1 (**Figure 7b**), which matches the value expected for Fp-PVBC. The FTIR and  $^1\text{H}$  NMR spectra for Fp-PVBC indicate that PVBC was fully functionalized by the Fp complexes, but the resulting products were not stable due to the formation of cross-linked material during precipitation.

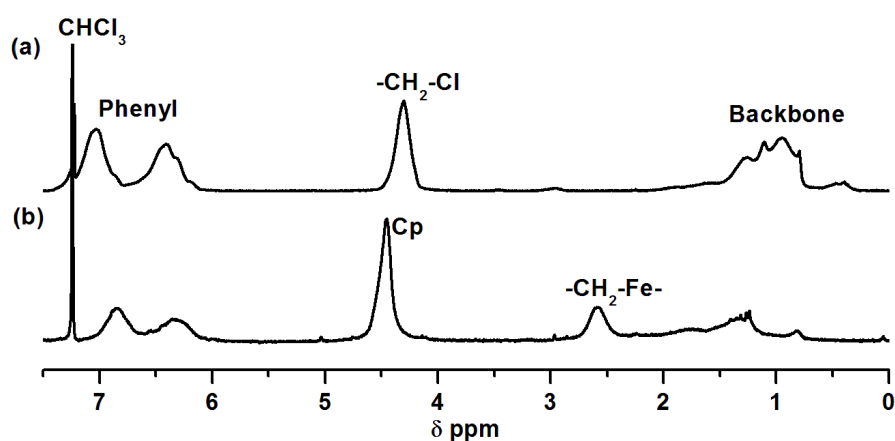
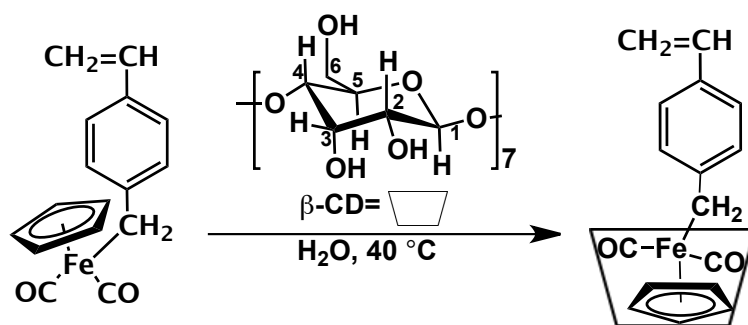


**Figure 7.**  $^1\text{H}$  NMR spectra ( $\text{CDCl}_3$ ) for PVBC (a) and Fp-PVBC (b).

### 3.2 Synthesis of $\beta$ -CD/Fp-VBC

It has been reported that the stability of organic and organometallic molecules can be significantly improved by host-guest interaction with CDs.<sup>[28,32,36-38,40,42]</sup> Therefore, we anticipated that host-guest chemistry of CDs could be used to improve the stability of Fp-PVBC and resolve the cross-linking problem that occurred during its precipitation. To assess this idea, we first prepared and characterized  $\beta$ -CD-complexed Fp-VBC ( $\beta$ -CD/Fp-VBC).  $\beta$ -CD/Fp-VBC was prepared by vigorously stirring  $\beta$ -CD and Fp-VBC in water at 40 °C (**Scheme 12**). After purification and freeze-drying, a pale yellow solid was collected (**Figure 8a**) and stored in the dark at low temperature (*ca.* 4 °C) to prevent possible auto-polymerization due to the high reactivity of the vinyl group on Fp-VBC. While Fp-VBC is soluble in most organic solvents, *e.g.*, THF, toluene, DCM and DMSO,<sup>[9]</sup>  $\beta$ -CD/Fp-VBC is only soluble in DMSO and dimethylformamide (DMF). Changes in solubility are commonly observed for CD inclusion compounds.<sup>[28,32,39]</sup>



**Scheme 12.** Synthesis of  $\beta$ -CD/Fp-VBC in water.

Fp-VBC is unstable in both solid and solution states in contact with air.<sup>[9]</sup> However, the  $\beta$ -CD-complexed Fp-VBC solid and its solution could be stored in air for over one month without detectable degradation. **Figure 8b** displays photographs for DMSO solutions of Fp-VBC and its  $\beta$ -CD inclusion compound after storage in air for over one month. The color of the Fp-VBC solution changed from yellow to brown and a precipitate was observed at the bottom of the tube (**Figure 8b**), which was due to degradation of the molecules. This decomposition was also confirmed by  $^1\text{H}$  NMR analysis. In contrast, the color of the  $\beta$ -CD/Fp-VBC solution displayed no obvious change over one month (**Figure 8b**), indicating that the chemical stability of Fp-VBC was improved by host-guest interactions with  $\beta$ -CDs.

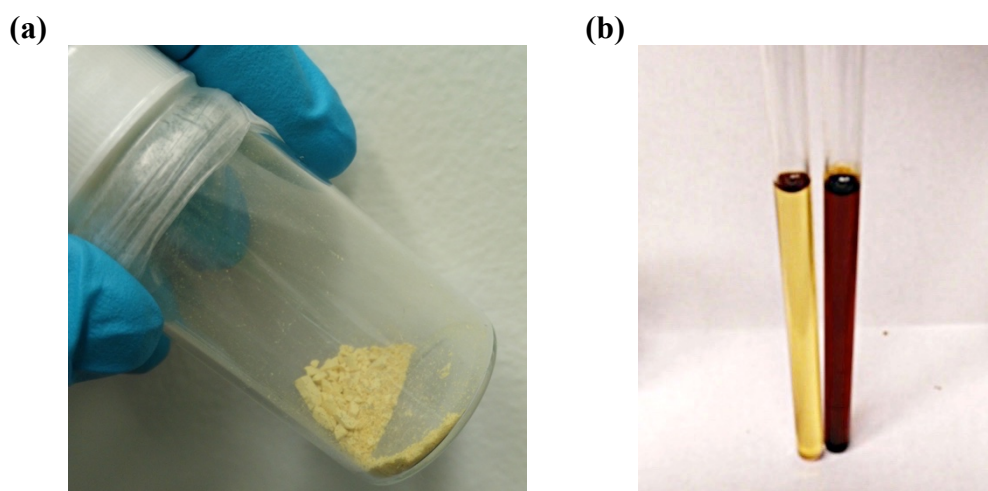


**Figure 8. Photographs for  $\beta$ -CD/Fp-VBC solids (a); DMSO solutions of  $\beta$ -CD/Fp-VBC (left) and Fp-VBC (right) after storing in air for one month (b).**

The thermal stability of  $\beta$ -CD, Fp-VBC and its  $\beta$ -CD inclusion compound was investigated by TGA. **Figure 9** shows that Fp-VBC starts to lose weight at *ca.* 140 °C due to the degradation of the Fp groups, and its second weight-loss stage at *ca.* 420 °C is due to the decomposition of the vinylbenzyl groups.<sup>[38,42,56]</sup>  $\beta$ -CD decomposes at *ca.* 300 °C.<sup>[40]</sup>  $\beta$ -CD/Fp-VBC shows no decomposition below 140 °C except the loss of hydration water. It is stable up to *ca.* 200 °C. This enhancement in thermal stability of  $\beta$ -CD/Fp-VBC is attributed to tight inclusion of the Fp group within the cavity of  $\beta$ -CD.<sup>[38,47]</sup>

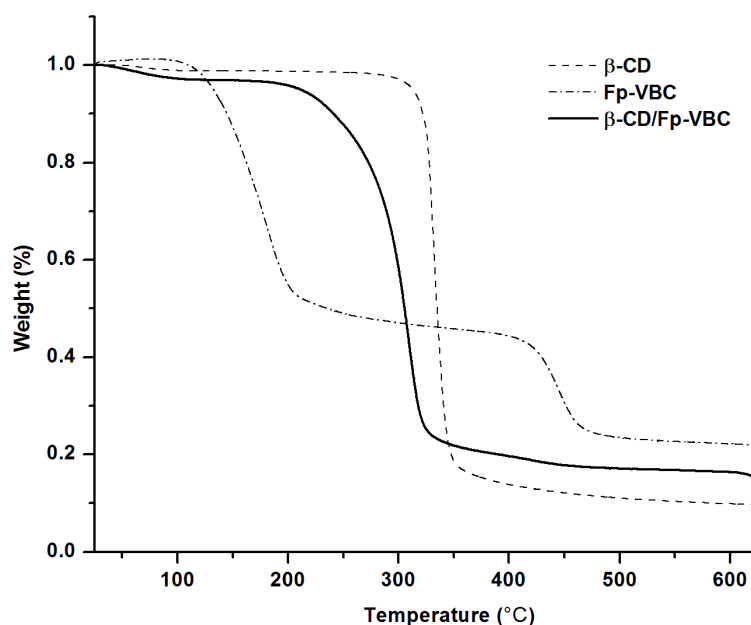


**Figure 9.** TGA curves for  $\beta$ -CD/Fp-VBC (solid line),  $\beta$ -CD (dashed line) and Fp-VBC (dash dotted line).

**Figure 10** illustrates the FTIR spectra for  $\beta$ -CD, Fp-VBC and  $\beta$ -CD/Fp-VBC. As shown in **Figure 10a**, Fp-VBC shows two strong absorptions at frequencies of 1996  $\text{cm}^{-1}$  and 1932  $\text{cm}^{-1}$ , corresponding to the terminal CO groups. Upon formation of the  $\beta$ -CD inclusion compounds, these two peaks shift slightly to 2007  $\text{cm}^{-1}$  and 1953  $\text{cm}^{-1}$  (**Figure 10b**) and the spectrum also displayed characteristic signals due to  $\beta$ -CDs, supporting the complexation of  $\beta$ -CD with Fp-VBC.<sup>[38-39]</sup>

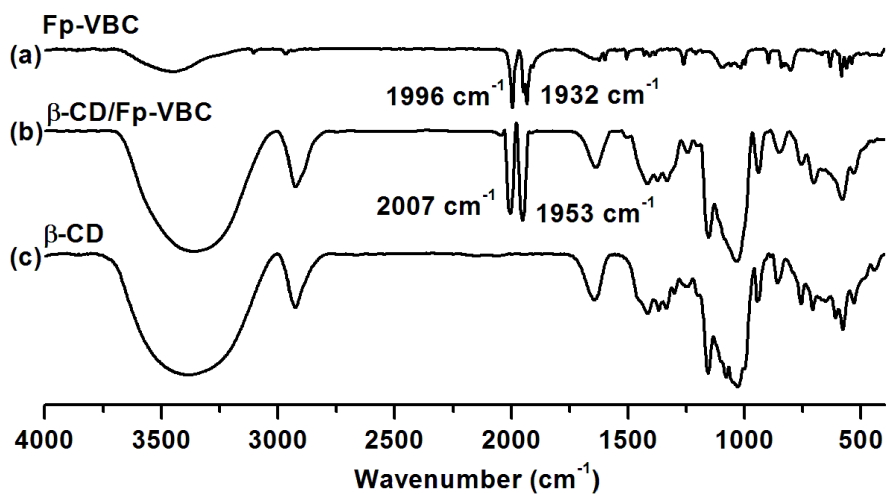


**Figure 10.** FTIR spectra for Fp-VBC (a), β-CD/Fp-VBC (b), β-CD (c).

<sup>1</sup>H NMR spectra for β-CD (a), Fp-VBC (b) and β-CD/Fp-VBC (c) in DMSO-*d*<sub>6</sub> are provided in **Figure 11**. Signals due to the protons of both β-CD (**Figure 11a**) and Fp-VBC (**Figure 11b**) are observed in the spectrum for β-CD/Fp-VBC (**Figure 11c**). The CD inclusion does not cause obvious shifts in these signals.<sup>[28,39-41,47]</sup> The integration ratios for these peaks are consistent with the theoretical values expected for the chemical structure of β-CD/Fp-VBC shown in **Scheme 12**. For example, the integration ratio of the signal due to the *Cp* rings to the signal due to the *phenyl* groups is 1.17:1, which is approximate to 5:4, and the integration ratio of the signal for the *Cp* rings to the signal for the *H*-1 protons in β-CDs is 1:1.51, which is

approximate 5:7. These ratios confirm that  $\beta$ -CD forms a 1:1 inclusion compound with Fp-VBC.

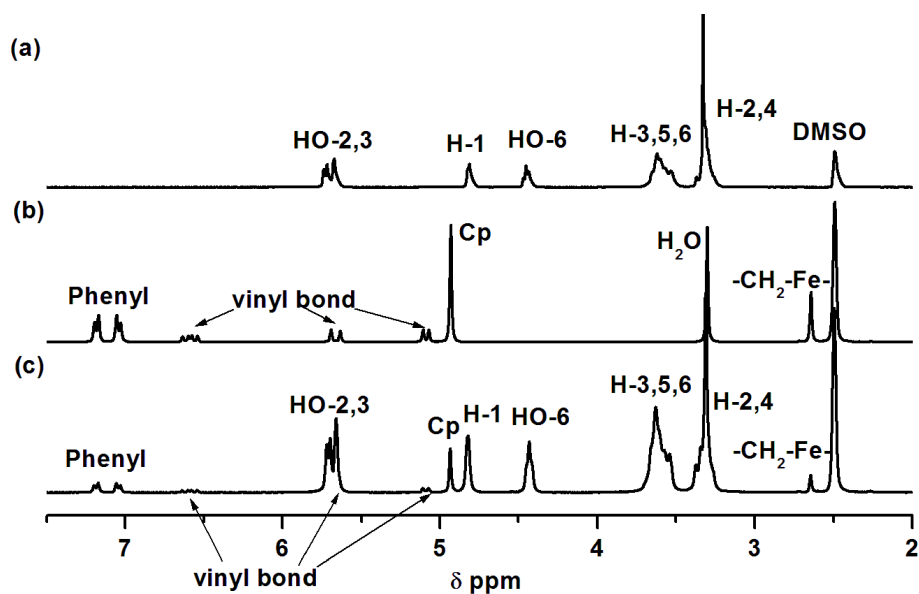
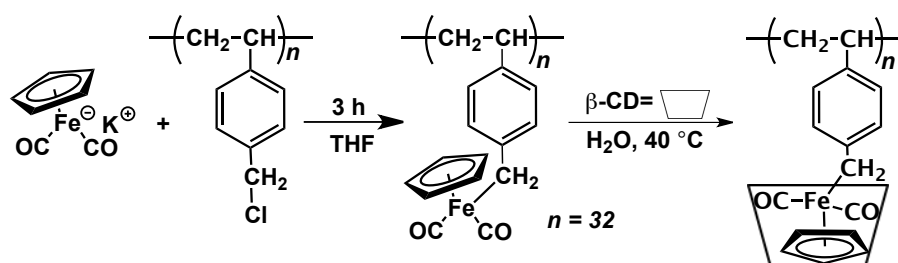


Figure 11.  $^1\text{H}$  NMR spectra ( $\text{DMSO-}d_6$ ) for  $\beta$ -CD (a), Fp-VBC (b),  $\beta$ -CD/Fp-VBC (c).

### 3.3 Synthesis of $\beta$ -CD/Fp-PVBC

To improve the stability of Fp-PVBC, we added an aqueous solution of  $\beta$ -CDs to the concentrated THF solution of Fp-PVBC before precipitation (**Scheme 13**). Upon addition of  $\beta$ -CD, a yellow solid gradually precipitated out. The color of the precipitate slowly turned to dark yellow, and eventually reddish. After purification, a reddish solid (**Figure 12a**) was collected. This solid was soluble in DMSO or DMF,

but not in other organic solvents, *e.g.*, THF, DCM, toluene. Importantly, the products could undergo repeated cycles of precipitation and dissolution in air, using DMSO as a good solvent and water as a non-solvent. No cross-linked material was generated during these cycles. The reddish product was assumed to be  $\beta$ -CD/Fp-PVBC as shown in **Scheme 13**.



**Scheme 13.** Synthesis of  $\beta$ -CD/Fp-PVBC.

As shown in **Figure 12b**, the DMSO solution of  $\beta$ -CD/Fp-PVBC displayed no obvious color change and did not precipitate after storing in air for over one month. In contrast, under the same conditions, the color of the Fp-PVBC solution turned from yellow to dark yellow, and eventually a brown precipitate was observed. This confirms that  $\beta$ -CD inclusion can improve the stability of Fp-PVBC.

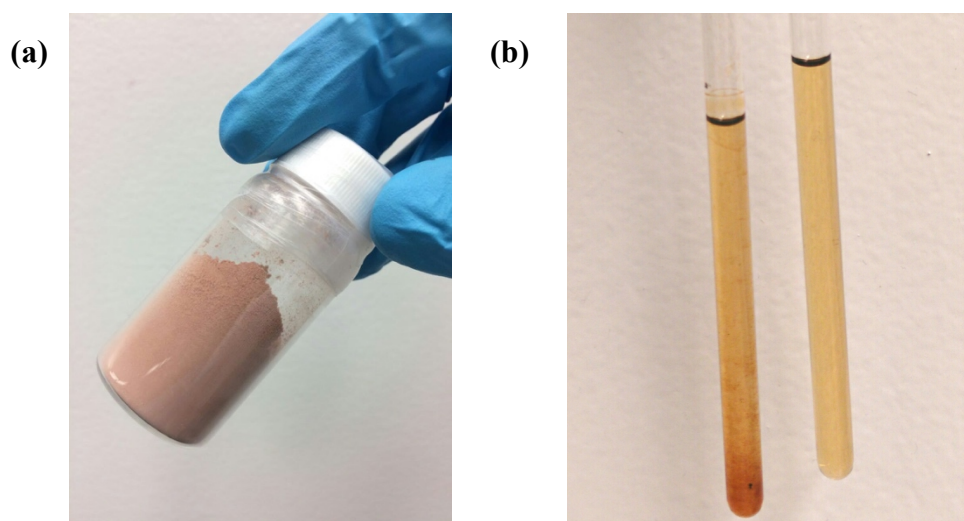


**Figure 12. Photographs for  $\beta$ -CD/Fp-PVBC solids (a); DMSO solutions of Fp-PVBC (left) and  $\beta$ -CD/Fp-PVBC (right) after storing in air for one month.**

The thermal stability of Fp-PVBC and  $\beta$ -CD/Fp-PVBC was investigated by TGA. As shown in **Figure 13**, Fp-PVBC, containing cross-linked material, shows two stages of weight loss. It starts to decompose at *ca.* 140 °C, which is attributed to the decomposition of the Fp groups, and a second weight loss starts at *ca.* 420 °C is due to the degradation of the polymer main-chain.<sup>[38,42,56]</sup>  $\beta$ -CD/Fp-PVBC was stable up to *ca.* 200 °C, and there is no decomposition at 140 °C. A slight weight loss above 100 °C is attributed to dehydration. Therefore, the thermal stability of

$\beta$ -CD/Fp-PVBC is improved by host-guest interactions of  $\beta$ -CD with the Fp group.<sup>[38,47]</sup>

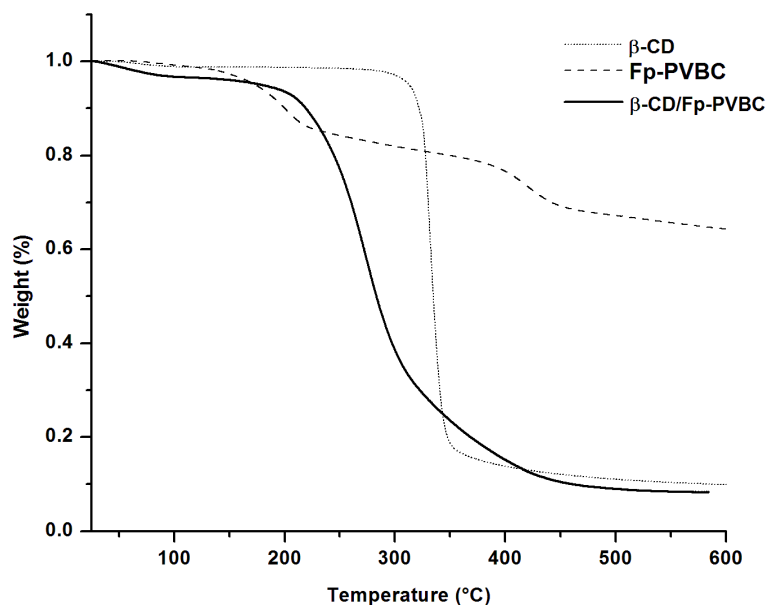


**Figure 13.** TGA curves for  $\beta$ -CD/Fp-PVBC (solid line),  $\beta$ -CD (dotted line) and Fp-PVBC (dashed line). note: Fp-PVBC contained cross-linked fractions.

**Figure 14b** provides the  $^1\text{H}$  NMR spectra for  $\beta$ -CD/Fp-PVBC in  $\text{DMSO-}d_6$ . Both signals due to the protons of Fp-PVBC (**Figure 14a**) and  $\beta$ -CDs (**Figure 11a**) are observed in the spectrum (**Figure 14b**), suggesting that complexation of  $\beta$ -CD with Fp-PVBC occurred.  $^{13}\text{C}$ - $^1\text{H}$  HMQC 2D NMR spectroscopy was performed to confirm the signal assignments for  $\beta$ -CD/Fp-PVBC. As shown in **Figure 15**, the signals for

the carbons and protons in  $\beta$ -CD, and their corresponding cross peaks are all observed.

The peak at 88.59 ppm in the  $^{13}\text{C}$  NMR spectrum is due to the carbons in the *Cp* rings, which correlates to the peak at 4.99 ppm in the  $^1\text{H}$  NMR spectrum. Meanwhile, the proton signal at 2.29 ppm due to the  $-\text{CH}_2\text{-Fe-}$  groups correlates to its carbon peak at 21.07 ppm. Four peaks at 137.35, 128.88, 128.20 and 125.32 ppm due to the carbons in the *phenyl* groups show cross peaks with the proton signals at 7.17-7.24 ppm.<sup>[13,17]</sup>

While the signals due to the protons in the polymer backbone are very weak, these peaks are visible in the expanded  $^1\text{H}$  NMR spectrum. However, the corresponding peaks in the  $^{13}\text{C}$  NMR spectrum are too weak to be observed. The weak signals for the polymer backbone are probably due to the enhanced rigidity of the polymer chains upon complexation of the Fp groups with bulky CD molecules.

The integration ratios for the protons due to the groups in the polymer side-groups are consistent with their theoretical values for the chemical structure shown in **Scheme 13**.

For example, the integration ratio for the peak due to the *Cp* rings to the peak due to the *phenyl* groups is 1.12:1 which is approximate 5:4. The integration ratio for the

peak due to the *Cp* rings to the peak due to the *H*-1 protons in  $\beta$ -CDs is 1:1.47 which is approximate 5:7. These integration ratios indicate that each Fp group interacts with one  $\beta$ -CD molecule, forming a 1:1 inclusion complex.

Nevertheless, the peaks due to the *Cp* rings (4.99 ppm) and the  $-\text{CH}_2\text{-Fe-}$  groups (2.29 ppm) in  $\beta$ -CD/Fp-PVBC (**Figure 14b**) shift substantially when compared with those (4.69 ppm and 2.72 ppm, respectively) in Fp-PVBC (**Figure 14a**). This difference suggests that the chemical environment of the  $\beta$ -CD complexed Fp groups in  $\beta$ -CD/Fp-PVBC is different from that in  $\beta$ -CD/Fp-VBC.

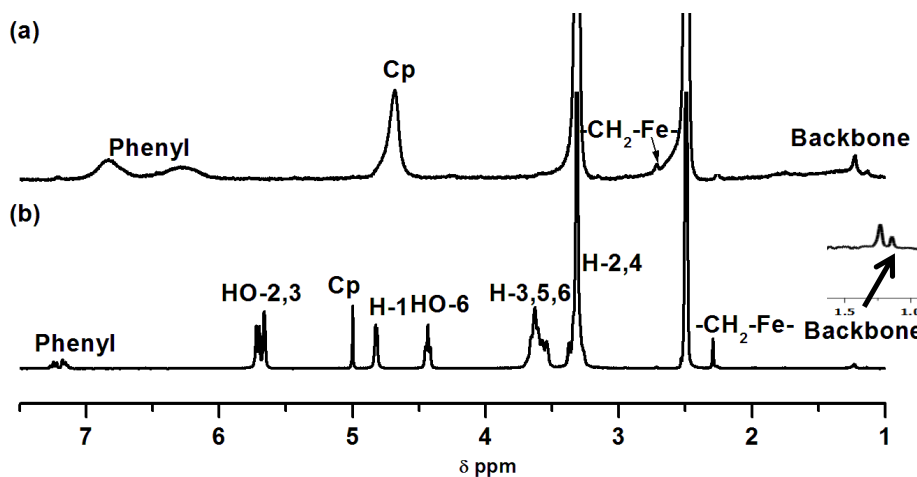


**Figure 14.**  $^1\text{H}$  NMR spectra ( $\text{DMSO-}d_6$ ) for Fp-PVBC (a) and  $\beta$ -CD/Fp-PVBC (b).

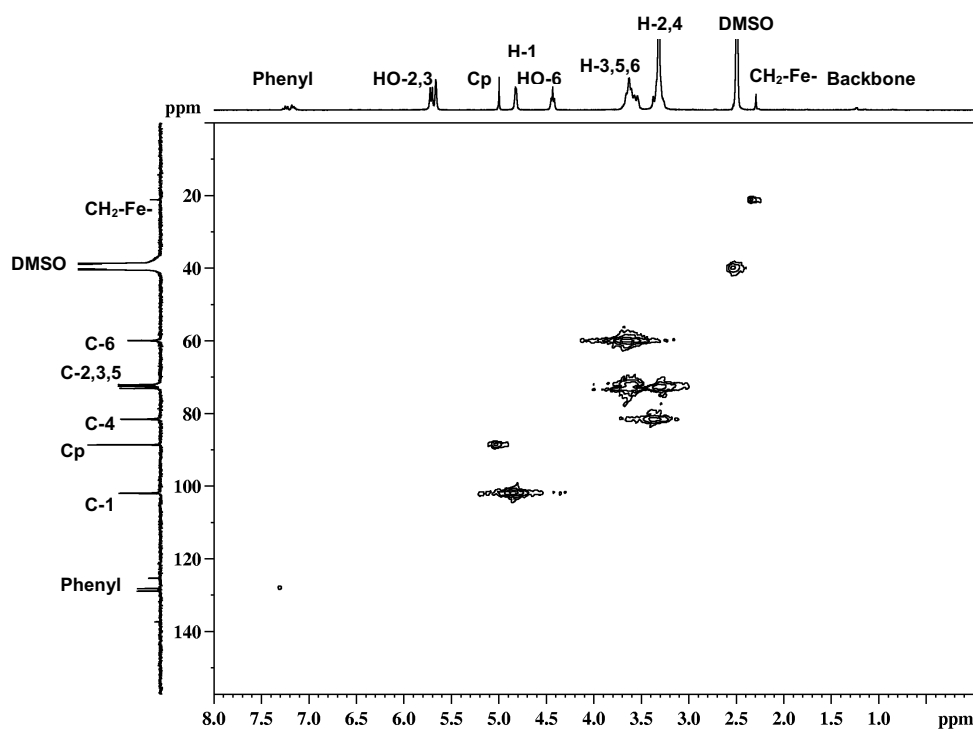
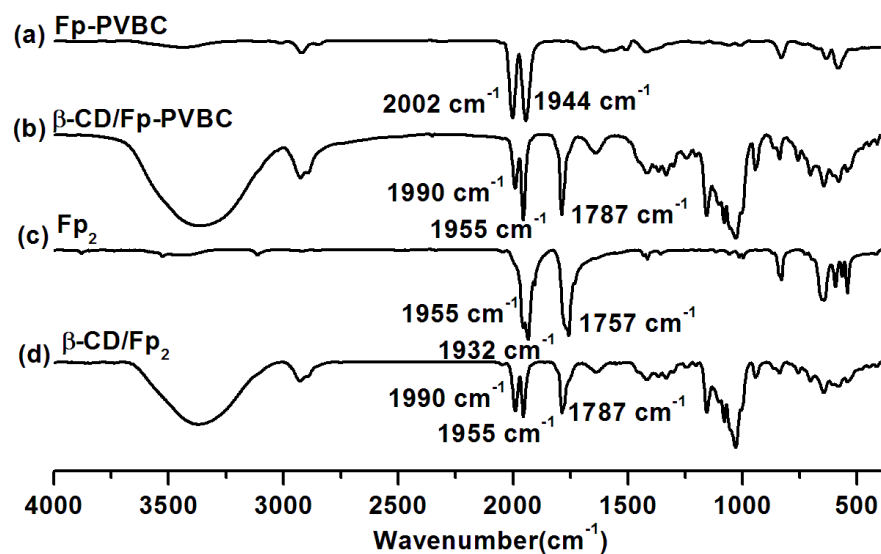


Figure 15.  $^{13}\text{C}$ - $^1\text{H}$  HMQC 2D NMR spectrum for  $\beta$ -CD/Fp-PVBC in  $\text{DMSO-}d_6$ .

FTIR spectroscopy was used to clarify the chemical structure of  $\beta$ -CD/Fp-PVBC. As shown in **Figure 16b**, upon inclusion within  $\beta$ -CD, the two absorption peaks due to the terminal CO groups in Fp-PVBC shift slightly from  $2002\text{ cm}^{-1}$  and  $1944\text{ cm}^{-1}$  (**Figure 16a**) to  $1990\text{ cm}^{-1}$  and  $1955\text{ cm}^{-1}$ , respectively. In addition, a new absorption peak is observed at  $1787\text{ cm}^{-1}$ . This absorption frequency is assigned to bridging CO groups, indicating the presence of Fp dimers.<sup>[54]</sup> In the case of  $\beta$ -CD/Fp-VBC, the FTIR spectrum shows no peaks for bridging CO ligands (**Figure 10b**). Therefore,

dimerization of the Fp groups may occur during the CD inclusion reaction of Fp-PVBC, and the chemical structure for  $\beta$ -CD/Fp-PVBC is speculated as shown in

**Figure 17.**



**Figure 16.** FTIR spectra for Fp-PVBC (a),  $\beta$ -CD/Fp-PVBC (b), Fp<sub>2</sub> (c) and  $\beta$ -CD/Fp<sub>2</sub>

(d).

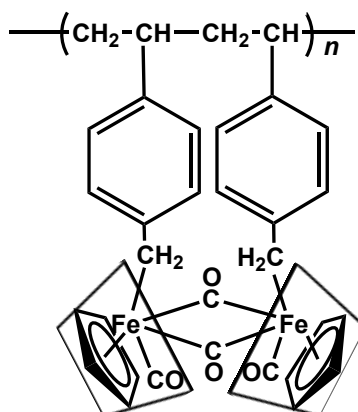
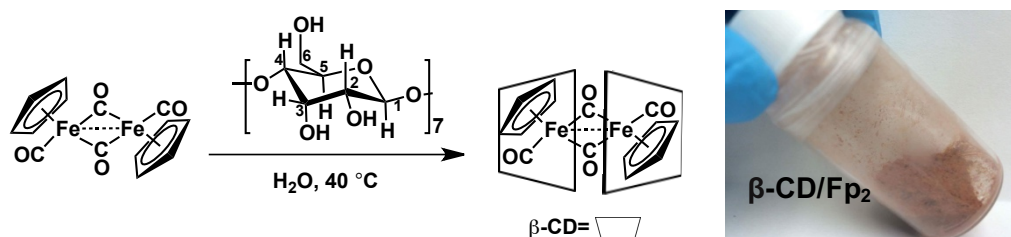


**Figure 17.** Proposed chemical structure for  $\beta$ -CD/Fp-PVBC.

To further confirm the presence of Fp dimers in  $\beta$ -CD/Fp-PVBC, we prepared  $\beta$ -CD complexed Fp<sub>2</sub> ( $\beta$ -CD/Fp<sub>2</sub>) (**Scheme 14**). The color of the  $\beta$ -CD/Fp<sub>2</sub> solids is reddish, which is similar to the color of  $\beta$ -CD/Fp-PVBC. As shown in **Figure 16c**, the FTIR spectrum for Fp<sub>2</sub> shows two peaks at 1955 cm<sup>-1</sup> and 1932 cm<sup>-1</sup> corresponding to the terminal CO ligands, and one peak at 1757 cm<sup>-1</sup> corresponding to the bridging CO ligands. Upon inclusion within  $\beta$ -CDs, these three peaks shift to 1990 cm<sup>-1</sup>, 1955 cm<sup>-1</sup> and 1787 cm<sup>-1</sup>, respectively (**Figure 16d**), which are the same absorption frequencies assigned to the terminal and bridging CO ligands for  $\beta$ -CD/Fp-PVBC (**Figure 16b**). These results support that the Fp groups on the polymer side-chains are dimerized (**Figure 17**).

The <sup>1</sup>H NMR spectra for  $\beta$ -CD/Fp-PVBC,  $\beta$ -CD/Fp-VBC and  $\beta$ -CD/Fp<sub>2</sub> are compared in **Figure 18**. The peaks due to the Cp rings for both  $\beta$ -CD/Fp-PVBC and  $\beta$ -CD/Fp<sub>2</sub> appear at 4.99 ppm (**Figure 18b, c**), but the peak due to the Cp rings for  $\beta$ -CD/Fp-VBC appears at 4.93 ppm (**Figure 18a**). This chemical shift difference

suggests that the structure of the Fp groups in  $\beta$ -CD/Fp-PVBC is similar to that in  $\beta$ -CD/Fp<sub>2</sub>.



**Scheme 14.** Synthesis of  $\beta$ -CD/Fp<sub>2</sub> in water.

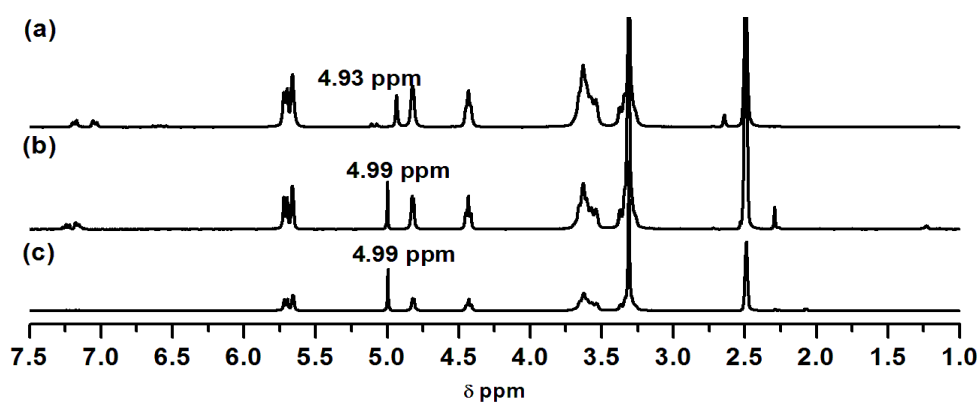


**Figure 18.** <sup>1</sup>H NMR spectra (DMSO-*d*<sub>6</sub>) for  $\beta$ -CD/Fp-VBC (a),  $\beta$ -CD/Fp-PVBC (b) and  $\beta$ -CD/Fp<sub>2</sub> (c).

Cyclic voltammetry (CV) is a useful technique to study MCPs, mostly due to the electroactive nature of the metal units.<sup>[57-58]</sup> The CV curves for DMSO solutions of Fp-VBC (a),  $\beta$ -CD/Fp-VBC (b), Fp-PVBC (c),  $\beta$ -CD/Fp-PVBC (d), Fp<sub>2</sub> (e) and

$\beta$ -CD/Fp<sub>2</sub> (f) are provided in **Figure 19**. Fp-VBC, Fp-PVBC and Fp<sub>2</sub> are electrochemically unstable and show irreversible redox cycles. Their corresponding  $\beta$ -CD inclusion complexes are anticipated to display better redox stability.<sup>[28,43]</sup> In the case of  $\beta$ -CD/Fp-PVBC and  $\beta$ -CD/Fp<sub>2</sub>, their redox cycles are reversible. Both cycles show one oxidation peak at *ca.* 0.80 V and one reduction peak at *ca.* -0.50 V. This similarity in redox behavior supports that  $\beta$ -CD/Fp-PVBC contains Fp dimers. The  $\beta$ -CD complexed Fp-VBC shows an irreversible redox cycle with two oxidation peaks at 0.6 V and 1.10 V, which is probably due to the lower electrochemical stability of the half-sandwich iron carbonyl complexes when compared with the symmetric dimer structures.<sup>[59]</sup> The absence of this electrochemical instability for  $\beta$ -CD/Fp-PVBC also suggests the presence of Fp dimers in the polymers.

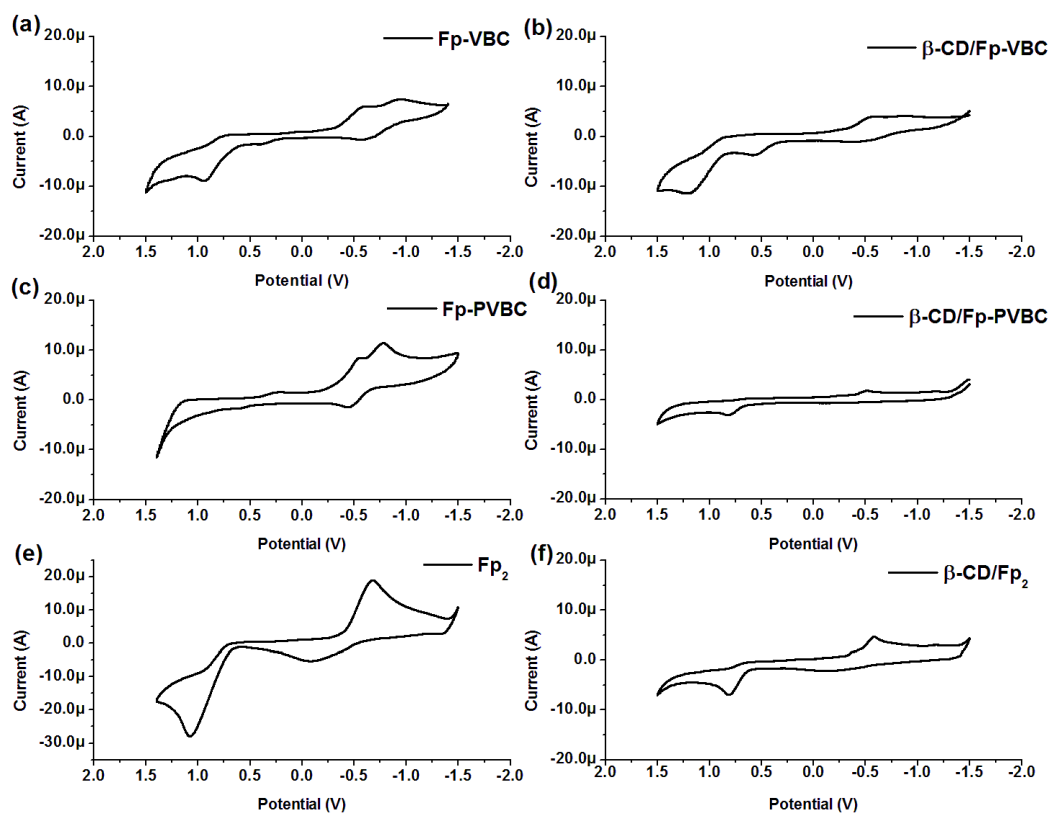
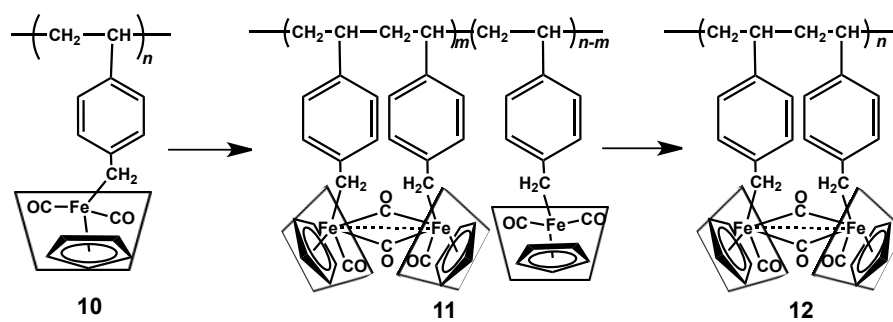


**Figure 19.** CV curves for Fp-VBC (a),  $\beta$ -CD/Fp-VBC (b), Fp-PVBC (c),  $\beta$ -CD/Fp-PVBC (d), Fp<sub>2</sub> (e) and  $\beta$ -CD/Fp<sub>2</sub> (f).

The dimerization process during the reaction is proposed in **Scheme 15**. After the addition of  $\beta$ -CD, the Fp groups were encapsulated into the cavities of  $\beta$ -CDs, resulting in a yellow precipitate (complexes **10**). These  $\beta$ -CD-complexed Fp groups underwent dimerization with the adjacent  $\beta$ -CD complexed Fp groups, and the color of the precipitates slowly turned to reddish due to the formation of complex **12**. Steric hindrance between the  $\beta$ -CD-complexed Fp groups is probably one reason for the

dimerization. In addition, it is reported that Fp groups are more stable in the dimer structures than in the half-sandwich structures.<sup>[54,60]</sup> This is also a favorable factor for dimerization.



**Scheme 15. Proposed dimerization process for the Fp groups on Fp-PVBC after the addition of  $\beta$ -CD.**

## 4. Conclusions

We first prepared Fp-PVBC by the post-polymerization modification of PVBC with Fp anions, but the resulting Fp-PVBC was not stable and partially cross-linked during precipitation. When  $\beta$ -CD was used to complex with the Fp groups, the stability of Fp-PVBC was significantly improved. The resulting  $\beta$ -CD/Fp-PVBC was stable in both solid and solution states. The electrochemical and thermal stability were also improved. According to the NMR, FTIR and CV analyses, the Fp groups on Fp-PVBC underwent dimerization with the adjacent Fp groups *via* CO bridging during the CD inclusion reaction.

## 5. Future Work

Although the chemical structure of  $\beta$ -CD/Fp-PVBC has been characterized, the molecular weight of  $\beta$ -CD/Fp-PVBC has not been measured. GPC or static light scattering (SLS) measurement should be used to characterize its molecular weight.

We can release the Fp groups from the cavities of  $\beta$ -CDs to produce uncomplexed Fp-PVBC. The Fp groups on the polymer side-chains are dimerized, so uncomplexed Fp-PVBC is expected to be stable enough for various characterization techniques. As discussed in the introduction, Ada derivatives can form more stable inclusion compounds with  $\beta$ -CDs than the Fc derivatives. Therefore, Ada derivatives, as the guest molecules, can be added to the solution of  $\beta$ -CD/Fp-PVBC to compete with the Fp groups, producing uncomplexed Fp-PVBC.

Furthermore, according to the idea that CDs can improve the stability of iron carbonyl polymers, MCPs with different metal units, *e.g.* molybdenum, ruthenium or tungsten,

can also be prepared *via* host-guest interaction with CDs, which could be important to the development of functional materials.

## References

- [1] C. G. Hardy, J. Zhang, Y. Yan, L. Ren and C. Tang, *Prog. Polym. Sci.* **2014**, *39*, 1742-1796.
- [2] Z. M. Al-Badri, R. R. Maddikeri, Y. Zha, H. D. Thaker, P. Dobriyal, R. Shunmugam, T. P. Russell and G. N. Tew, *Nat. Commun.* **2011**, *2*, 482.
- [3] U. Hasegawa, A. J. van der Vlies, E. Simeoni, C. Wandrey and J. A. Hubbell, *J. Am. Chem. Soc.* **2010**, *132*, 18273-18280.
- [4] G. R. Whittell and I. Manners, *Adv. Mater.* **2007**, *19*, 3439-3468.
- [5] D. A. Poulsen, B. J. Kim, B. Ma, C. S. Zonte and J. M. J. Fréchet, *Adv. Mater.* **2010**, *22*, 77-82.
- [6] R. G. H. Lammertink, M. A. Hempenius, J. E. van den Enk, V. Z. H. Chan, E. L. Thomas and G. J. Vancso, *Adv. Mater.* **2000**, *12*, 98-103.
- [7] M. Burnworth, L. Tang, J. R. Kumpfer, A. J. Duncan, F. L. Beyer, G. L. Fiore, S. J. Rowan and C. Weder, *Nature* **2011**, *472*, 334-337.
- [8] L. A. Míinea, L. B. Sessions, K. D. Ericson, D. S. Glueck and R. B. Grubbs, *Macromolecules* **2004**, *37*, 8967-8972.

- [9] S. Kher and T. Nile, *Transition Met. Chem.* **1991**, *16*, 28-30.
- [10] H. K. Sharma, F. Cervantes-Lee and K. H. Pannell, *J. Am. Chem. Soc.* **2004**, *126*, 1326-1327.
- [11] G. Shultz and D. Tyler, *J. Inorg. Organomet. Polym. Mater.* **2009**, *19*, 423-435.
- [12] W. Y. Chan, S. B. Clendenning, A. Berenbaum, A. J. Lough, S. Aouba, H. E. Ruda and I. Manners, *J. Am. Chem. Soc.* **2005**, *127*, 1765-1772.
- [13] J. Liu, K. Cao, B. Nayyar, X. Tian and X. Wang, *Polym. Chem.* **2014**, *5*, 6702-6709.
- [14] H. Braunschweig, T. Dellermann, R. D. Dewhurst, J. Mies, K. Radacki, S. Stellwag-Konertz and A. Vargas, *Organometallics* **2014**, *33*, 1536-1539.
- [15] D. R. Tyler, *Coord. Chem. Rev.* **2003**, *246*, 291-303.
- [16] D. R. Tyler, *Inorg. Chim. Acta* **2015**, *424*, 29-37.
- [17] X. Wang, K. Cao, Y. Liu, B. Tsang and S. Liew, *J. Am. Chem. Soc.* **2013**, *135*, 3399-3402.
- [18] C. Pittman, Jr., *J. Inorg. Organomet. Polym. Mater.* **2005**, *15*, 33-55.
- [19] A. K. Saha and M. M. Hossain, *J. Organomet. Chem.* **1993**, *445*, 137-141.

- [20] S. F. Mapolie, I. J. Mavunkal, J. R. Moss and G. S. Smith, *Appl. Organomet. Chem.* **2002**, *16*, 307-314.
- [21] Y. Morisaki, H. Chen and Y. Chujo, *Polym. Bull.* **2002**, *48*, 243-249.
- [22] C. U. Pittman, G. V. Marlin and T. D. Rounsefell, *Macromolecules* **1973**, *6*, 1-8.
- [23] C. U. Pittman and R. F. Felis, *J. Organomet. Chem.* **1974**, *72*, 399-413.
- [24] M. V. Rekharsky and Y. Inoue, *Chem. Rev.* **1998**, *98*, 1875-1918.
- [25] B.-w. Liu, H. Zhou, S.-T. Zhou and J.-Y. Yuan, *Eur. Polym. J.* **2015**, *65*, 63-81.
- [26] F. Hapiot, S. Tilloy and E. Monflier, *Chem. Rev.* **2006**, *106*, 767-781.
- [27] H. Ritter, O. Sadowski and E. Tepper, *Angew. Chem. Int. Ed.* **2003**, *42*, 3171-3173.
- [28] H. Ritter, B. E. Mondrzik, M. Rehahn and M. Gallei, *Beilstein J. Org. Chem.* **2010**, *6*, 60.
- [29] T. Matsue, D. H. Evans, T. Osa and N. Kobayashi, *J. Am. Chem. Soc.* **1985**, *107*, 3411-3417.
- [30] W. C. Cromwell, K. Bystrom and M. R. Eftink, *J. Phys. Chem.* **1985**, *89*, 326-332.
- [31] I. Yamamoto, T. Unai, Y. Suzuki and Y. Katsuda, *J. Pestic. Sci.* **1976**, *1*, 41-48.
- [32] W. Saenger, *Angew. Chem. Int. Ed.* **1980**, *19*, 344-362.

- [33] J. L. Lach and W. A. Pauli, *J. Pharm. Sci.* **1966**, *55*, 32-38.
- [34] K. Uekama, F. Hirayama, M. Otagiri, Y. Otagiri and K. E. N. Ikeda, *Chem. Pharm. Bull.* **1978**, *26*, 1162-1167.
- [35] T. Kinoshita, F. Linuma and A. Tsuji, *Biochem. Biophys. Res. Commun.* **1973**, *51*, 666-671.
- [36] S. Aime, M. R. Chierotti, R. Gobetto, A. Masic, F. Napolitano, H. C. Canuto and S. J. Heyes, *Eur. J. Inorg. Chem.* **2008**, *2008*, 152-157.
- [37] M. Shimada, A. Harada and S. Takahashi, *J. Chem. Soc., Chem. Commun.* **1991**, 263-264.
- [38] M. Shimada, Y. Morimoto and S. Takahashi, *J. Organomet. Chem.* **1993**, *443*, C8-C10.
- [39] P. P. Patel and M. E. Welker, *J. Organomet. Chem.* **1997**, *547*, 103-112.
- [40] F. Zuo, C. Luo, X. Ding, Z. Zheng, X. Cheng and Y. Peng, *Supramol. Chem.* **2008**, *20*, 559-564.
- [41] A. Harada and S. Takahashi, *J. Chem. Soc., Chem. Commun.* **1984**, 645-646.
- [42] S. S. Braga, F. A. Almeida Paz, M. Pillinger, J. D. Seixas, C. C. Romão and I. S.

- Gonçalves, *Eur. J. Inorg. Chem.* **2006**, 2006, 1662-1669.
- [43] M. Nakahata, Y. Takashima, H. Yamaguchi and A. Harada, *Nat. Commun.* **2011**, 2, 511.
- [44] Q. Yan, J. Yuan, Z. Cai, Y. Xin, Y. Kang and Y. Yin, *J. Am. Chem. Soc.* **2010**, 132, 9268-9270.
- [45] L. r. Pospíšil, M. Hromadová, J. Fiedler, C. Amatore and J.-N. Verpeaux, *J. Organomet. Chem.* **2003**, 668, 9-16.
- [46] L. X. Song, F. Y. Du, X. Q. Guo and S. Z. Pan, *J. Phys. Chem. B* **2010**, 114, 1738-1744.
- [47] A. Harada, Y. Hu, S. Yamamoto and S. Takahashi, *J. Chem. Soc., Dalton Trans.* **1988**, 729-732.
- [48] F. Huang and H. W. Gibson, *Prog. Polym. Sci.* **2005**, 30, 982-1018.
- [49] A. Harada, Y. Takashima and H. Yamaguchi, *Chem. Soc. Rev.* **2009**, 38, 875-882.
- [50] M. Wilhelm, C. L. Zhao, Y. Wang, R. Xu, M. A. Winnik, J. L. Mura, G. Riess and M. D. Croucher, *Macromolecules* **1991**, 24, 1033-1040.
- [51] S. Y. Cho and H. R. Allcock, *Macromolecules* **2009**, 42, 4484-4490.

- [52] J. T. Lai, D. Filla and R. Shea, *Macromolecules* **2002**, *35*, 6754-6756.
- [53] J. S. Plotkin and S. G. Shore, *Inorg. Chem.* **1981**, *20*, 284-285.
- [54] E. Mocellin, M. Ravera, R. A. Russell and T. Hynson, *J. Chem. Educ.* **1996**, *73*,  
A99.
- [55] K. Cao, J. Ward, R. C. Amos, M. G. Jeong, K. T. Kim, M. Gauthier, D. Foucher  
and X. Wang, *Chem. Commun.* **2014**, *50*, 10062-10065.
- [56] W. Lu, Z.-G. Shao, G. Zhang, Y. Zhao and B. Yi, *J. Power Sources* **2014**, *248*,  
905-914.
- [57] D. P. Puzzo, A. C. Arsenault, I. Manners and G. A. Ozin, *Angew. Chem. Int. Ed.*  
**2009**, *48*, 943-947.
- [58] R. Rulkens, A. J. Lough, I. Manners, S. R. Lovelace, C. Grant and W. E. Geiger, *J.*  
*Am. Chem. Soc.* **1996**, *118*, 12683-12695.
- [59] M. Kumar, F. Cervantes-Lee, K. H. Pannell and J. Shao, *Organometallics* **2008**, *27*,  
4739-4748.
- [60] R. D. Theys, M. E. Dudley and M. M. Hossain, *Coord. Chem. Rev.* **2009**, *253*,  
180-234.

[61] T. Uyar, M. A. Hunt, H. S. Gracz and A. E. Tonelli, *Cryst. Growth Des.* **2006**, *6*,

1113-1119.